Multi-Neuromodulator Measurements across Fronto-Striatal Network Areas of the Behaving Macaque using Solid-Phase Microextraction

Seyed-Alireza Hassani[1,2,†] , Sofia Lendor[3,†] , Ezel Boyaci[3], Janusz Pawliszyn[3,‡,] and Thilo Womelsdorf[1,2,‡,*]

1 Department of Psychology, Vanderbilt University, PMB 407817, 2301 Vanderbilt Place, Nashville TN 37240, USA
2 Department of Biology, Centre for Vision Research, York University, Toronto, Ontario M6J 1P3, Canada
3 Department of Chemistry, University of Waterloo, 200 University Avenue West, Waterloo, Ontario N2L 3G1, Canada

* Corresponding author: Thilo Womelsdorf Tel. 615-322-0070, E-mail: thilo.womelsdorf@vanderbilt.edu
† ‡ These authors contributed equally

Short title: Sensing of multiple neurotransmitters in-vivo using SPME

Abstract

Different neuromodulators rarely act independent from each other to modify neural processes but are instead co-released, gated, or modulated. To understand this interdependence of neuromodulators and their collective influence on local circuits during different brain states, it is necessary to reliably extract local concentrations of multiple neuromodulators in vivo. Here we describe results using solid phase microextraction (SPME), a method providing sensitive, multi-neuromodulator measurements. SPME is a sampling method that is coupled with mass spectrometry to quantify collected analytes. Reliable measurements of glutamate, dopamine, acetylcholine and choline were made simultaneously within frontal cortex and striatum of two macaque monkeys (*Macaca mulatta*) during goal-directed behavior. We find glutamate concentrations several orders of magnitude higher than acetylcholine and dopamine in all brain regions. Dopamine was reliably detected in the striatum at tenfold higher concentrations than acetylcholine. Acetylcholine and choline concentrations were detected with high consistency across brain areas, within monkeys and between monkeys. These findings illustrate that SPME microprobes provide a versatile novel tool to characterize multiple neuromodulators across different brain areas in vivo to understand the interdependence and co-variation of neuromodulators during goal directed behavior. Such data will be important to better distinguish between different behavioral states and characterize dysfunctional brain states that may be evident in psychiatric disorders.

Introduction

50 Extracellular concentrations of neuromodulators influence firing regimes, input-output
51 relationships and neural interactions in local circuits and long-range brain networks (Marder 2012;
52 Thiele and Bellgrove 2018), and are dysregulated in virtually all psychiatric disorders (Avery and
53 Krichmar 2017; Millan et al. 2012). Accumulating evidence suggests that these fundamental roles
54 of neuromodulators for circuit functioning are unlikely realized by single neuromodulators
55 operating in isolation. Rather, neuromodulatory systems are heavily intertwined (Avery and
56 Krichmar 2017; Gobert et al. 1998; Moehle et al. 2017), and operate simultaneously on individual
57 cells and circuits (Arnsten et al. 2010; Hassan et al. 2015; Marder 2012; Santana et al. 2018). In
58 each circuit, local mechanisms exert control over the release of neuromodulators from terminals
59 of brainstem-originating projection neurons. This local control proceeds through activation of pre-
60 synaptic glutamatergic receptors (Ghersi et al. 2003; Grilli et al. 2009; Luccini et al. 2007; Pittaluga
61 2016; Pittaluga et al. 2006; Wang et al. 1992). These insights suggest that an understanding of the
62 contribution of neuromodulators to circuit functioning requires measuring, simultaneously,
63 multiple neuromodulators in conjunction with ongoing glutamatergic neurotransmitter
64 concentrations and action. Consistent with this conclusion single neuromodulator theories often
65 fail to account for all observable symptoms in psychiatric diseases (Bohnen et al. 2015; Halliday
66 et al. 2014; Remy et al. 2005).

67 Despite the accumulating evidence for the interdependence of neuromodulator actions, few
68 methods exist for their simultaneous measurement in vivo and across multiple brain areas (**Table**
69 **S1**). Most of these existing neurochemical sensing methods allowing multi-neuromodulator
70 sampling have a barrier to entry by requiring specialized equipment and trained experts preventing
71 data collection by scientists who are otherwise interested in the role of endogenous and exogenous
72 neuroactive chemicals in cognition and psychiatric disorders. Electrochemical methods such as

73 fast scan cyclic voltammetry (FSCV) and amperometry have sub-second temporal resolution, but
74 are limited to the measurement of a few compounds (Dale et al. 2005; Jacobs et al. 2010) and are
75 challenging and not robust for wide-spread in vivo application in nonhuman primates yet, although
76 several labs have recently reported success (Disney et al. 2015; König et al. 2018; Quintero et al.
77 2007; Schluter et al. 2014; Schwerdt et al. 2017; Vartak et al. 2017; Yoshimi et al. 2015). Imaging
78 techniques such as positron emission tomography (PET) are also limited to the measurement of
79 one or a few compounds simultaneously (Fisher et al. 1995). Microdialysis (MD) paired with mass
80 spectrometry is the most commonly used method for measuring multiple neuromodulators in
81 awake behaving animals. MD provides a data collection method which is then analyzed post hoc
82 to identify and quantify collected analytes. It operates with a semi-permeable membrane which
83 allows for the continuous collection of the available extracellular neuromodulators through passive
84 diffusion, and can even be used to locally release pharmacological agents (Anderzhanova and
85 Wotjak 2013; Buck et al. 2009; Kennedy 2013; Perry et al. 2009; Watson et al. 2006). However,
86 MD does have several disadvantages. MD disrupts the tissue during its initial placement of the
87 probe or a guiding cannula resulting in damage-induced release of neuromodulators that can last
88 several hours before stable measurements become possible. Moreover, MD has low affinity for
89 hydrophobic compounds and comparatively broad spatial and temporal resolution that is in the
90 range of 200-400 μm in diameter and 10-20 minutes, respectively. These values are dependent on
91 the surface area of the permeable membrane, the exact method of MD, flow rate, resolution of
92 detection methods for analytes of interest, tissue tortuosity and more (Anderzhanova and Wotjak
93 2013; Kennedy 2013; Watson et al. 2006).

94 Here, we set out to address some of these limitations with a novel protocol for measuring
95 multiple neuromodulators in vivo in discrete 20 minute intervals using probes optimized for solid

96 phase microextraction (SPME) (Pawliszyn 2000, 2012). SPME probes are thin (200 μm) wires of
97 arbitrary length coated with an inert porous polymeric matrix using biocompatible binder on one
98 end where molecules with appropriate size and affinity migrate via passive diffusion and are
99 retained by weak intermolecular interactions (*see* Methods). SPME provides an alternate method
100 for data collection which can then be analyzed by tools such as mass spectrometers. This method
101 has been shown to extract in neural tissue dynamic changes in dopamine (DA) and serotonin (5-
102 HT) levels with comparable precision to MD (Cudjoe et al. 2013; Cudjoe and Pawliszyn 2014).
103 Additionally, due to the similarity of SPME probes to commonly used microelectrodes in
104 electrophysiological recordings, relatively minor adjustments will allow for the adaptation of
105 conventional microelectrode driving systems for SPME use. This, combined with post collection
106 analysis through standard chemistry facilities makes SPME an attractive and easy-to-use tool for
107 electrophysiology labs.

108 SPME has the potential to be a powerful new tool to compliment the mentioned methods
109 well suited for neurochemical profiling that spans both multiple neuromodulators as well as
110 multiple brain regions simultaneously. Such data will allow for global observation of slow
111 neuromodulator dynamics that could better inform our hypotheses and help relate global
112 neuromodulator levels to electrophysiology and behavior.

113 Thus, the ability of SPME to report major neuromodulators as well as glutamate and GABA
114 were tested in two behaving rhesus macaques. Probes were repeatedly and simultaneously inserted
115 into two cortical regions and the striatum to observe inter-areal differences between extracellular
116 neuromodulator concentrations. We found that extracellular concentrations of glutamate,
117 dopamine, acetylcholine and choline could be reliably distinguished and differed systematically
118 between brain regions.

Methods

Animals

Data was collected from two 8 year-old male rhesus macaques (*Macaca mulatta*) weighing 8-12 kg. All animal care and experimental protocols were approved by the York University Animal Care Committee and were in accordance with the Canadian Council on Animal Care guidelines. Details regarding the experimental setup, recording procedures, and reconstruction of recording sites have been described previously (Oemisch et al. 2015). Briefly, animals were implanted with a 20 mm by 28 mm recording chamber over the frontal region of the right hemisphere guided by stereotaxic coordinates (Paxinos et al. 2000) and MR images. The animals were seated in a custom made primate chair and head stabilized with their eyes 65cm away from a 21' LCD monitor refreshed at 85 Hz. Eye traces were collected by a video-based eye-tracking system (Eyelink 1000 Osgoode, Ontario, Canada, 500 Hz sampling rate). The animals were engaged in an over-trained attention tasks in which they would use saccadic eye movements to acquire juice reward (**Fig S1**). The specifics of the task are described elsewhere (Hassani et al. 2017). Both animals showed stable performance and acquired similar reward volumes on all recording days. In both tasks, stimulus presentation and reward delivery was controlled through MonkeyLogic (http://www.brown.edu/Research/monkeylogic/).

SPME protocol and Fabrication of SPME Probes

We provide a visual overview of the complete SPME protocol used here in **Fig S2** and delineate the chemical materials, LC-MS/MS analysis, and detailed quantitation of neuromodulators in the ***Supplementary Materials*** and in a companion paper (Lendor et al. 2019). All measurements used miniaturized SPME probes that were manufactured by repeated dip-coating of stainless steel wires

142 in a suspension of extracting phase in a binder. This general procedure reported previously
143 (Gómez-Ríos et al. 2017), has been modified to fit the purpose of *in vivo* brain sampling (Lendor
144 et al. 2019). The 3 mm long tip of the wire was acid-etched down to approx. 100 μm to create a
145 recession capable of accommodating thicker layer of coating without significantly increasing the
146 total probe diameter. The extracting phase was an in-house synthesized hydrophilic-lipophilic
147 balance polymer functionalized with benzenesulfonic acid to introduce strong cation exchange
148 properties (HLB-SCX). The monodispersed polymeric particles with diameter of approx. 1 μm
149 were suspended in the binder consisting of 7% polyacrylonitrile dissolved in N,N-dimethylformide
150 (w/v), ensuring the particles-to-binder ratio at 15% (w/v). The extracting phase suspension was
151 prepared one day before the probe coating, homogenized by sonication and stirred at 800 rpm
152 overnight. Several layers of coating were deposited on the modified wires, resulting in total coating
153 thickness of ≈50 μm and total probe diameter of 195 μm. The average pore size of the extracting
154 phase was measured at 1.2nm. Before the use, the probes were cleaned with the mixture of
155 methanol, acetonitrile and 2-propanol (50:25:25, v/v/v), activated in the mixture of methanol and
156 water (50:50. v/v) and sterilized in steam for 15 min at 121°C. During the sampling, SPME probes
157 were inserted into sheathing cannulas to protect the coating and prevent it from extracting
158 compounds on the way to the target brain area. The cannulas underwent the same cleaning and
159 sterilization procedure as the probes and then the lengths of both components of the SPME
160 assembly were adjusted to 60-70 and 70-80 mm for the probes and cannulas, respectively.
161

162 **MRI Guided Electrophysiological Mapping of Target Tissue**

163 The anatomical coordinates of the brain regions of interest were first identified through 3 T MR
164 images. The MR images were then verified with extracellular electrophysiological recordings of

165 the target areas, which provided the gray and white matter boundaries for the cortical sites and the
166 dorsal most aspect of the head of the caudate nucleus. Tungsten microelectrodes were 200 μm
167 thick with an impedance of 1-2 MΩ. All electrodes, SPME probes and their accompanying guiding
168 cannulas were driven down into the brain and later out using software-controlled precision
169 microdrives (Neuronitek, ON, Canada). Electrodes were connected to a multichannel acquisition
170 processor (Neuralynx Digital Lynx system, Inc., Bozeman, Montana, USA) which was used for
171 data amplification, filtering and acquisition of spiking activity. Spiking activity was obtained by
172 applying a 600-8000 Hz bandpass filter, with further amplification and digitization at a 32 KHz
173 sampling rate. For every recording day, electrodes were lowered until the first detection of spiking
174 activity (indicative of gray matter) at the depth suggested by the MR images.
175
176 **SPME Sampling and Post-Processing Procedures**
177 All three SPME assemblies (example of sampling using one assembly in **Fig 1A-C**) were
178 simultaneously driven to 200 μm above the point of first spiking detection. SPME assemblies were
179 located ~1 mm away from the electrode penetration location. Then, only the SPME probes were
180 inserted 3 mm into the areas of interest. On average macaque cortical thickness is only 2 mm while
181 the head of the caudate at the point of sampling was well over 3 mm. An extraction duration of 20
182 min was selected to reflect stable extraction time profiles for all compounds of interest. The
183 kinetics of target analyte extraction, for example glutamate and dopamine, can be visualized in
184 vitro through extraction time profiles (Lendor et al. 2019) (**Fig 1D-E**). Brain homogenate was
185 spiked with known concentrations of target analytes and four replicates were collected during
186 which multiple probes were placed in the homogenate and sequentially removed at reported times
187 after initial insertion and quantified (LC-MS/MS procedure described below). These extraction

188 time profiles reflect the quantifiable concentration of collected analyte over time, which is captured
189 in sequence by a linear "kinetic" regime, a "dynamic" regime and an "equilibrium" regime over
190 extraction time. These labels are used to describe the various rates of analyte adsorption by the
191 SPME fibre, where the kinetic regime reflects the fastest adsorbtion of the target analyte, the
192 equilibrium regime reflects a period of only marginal further analyte collection and an intermediate
193 dynamic regime (Ouyang and Pawliszyn 2007). These extraction kinetics provide information
194 about the time it takes until equilibrium is reached in a concentration independent manner that is
195 helpful in estimating a lower limit for extraction times to collect quantifiable analyte
196 concentrations. After the 20 min extraction event, all SPME probes were driven back 3 mm into
197 the guiding cannulas and all SPME assemblies were withdrawn from the brain (**Fig 1A-C**). The
198 microdrives were then removed from the chamber to enable unclamping of the SPME probes, a
199 brief wash and then storage in glass vials surrounded by dry ice until placing them into a -80°C
200 freezer. One entire sampling event (one extraction in 3 different brain areas together with
201 assembling the SPME probes and cannulas, driving into and out of brain, washing and preparing
202 for storage) was performed within 50 min, except for the first sampling event in each sampling
203 day. The first sampling event, with the area identification using electrophysiology recording, was
204 performed within 75 min. The removal of the SPME microprobe from the gray matter and the
205 positioning of a new SPME microprobe in the same location limits the temporal continuity of
206 sampling. We believe that further optimizing of the SPME microprobe switching procedure with
207 e.g. pre-loaded SPME probes will allow replacing SPME fibres within 2-10 min. Alternatively,
208 SPME microprobes could be used in spatially separate but adjacent guiding tubes (separation of
209 ~300μm), which would allow to switch sampling from one to other probe without temporal delays.
210

211 **Neuromodulator detection and quantitation**

212 Detection and quantitation of neuromodulators followed previously established procedures
213 described in the **Supplementary Materials**. In brief, SPME probes were defrosted and desorbed
214 in an aqueous solution containing water, acetonitrile, methanol, formic acid and deuterated
215 isotopologues of target neuromodulators as internal standards (IS). Chromatographic separation of
216 target compounds was conducted as previously reported (Cudjoe and Pawliszyn 2014). Tandem
217 mass spectrometry (MS/MS) was performed with electrospray ionization with two MS/MS
218 transitions for each neuromodulator and one for each IS (Lendor et al. 2019).

219 Stock solutions of all target neuromodulators were prepared and used to generate standard
220 calibration curves and to calculate the amounts of neuromodulator extracted by each experimental
221 SPME probe. Conversion of the amount of neuromodulator extracted to in-brain concentrations
222 was done using matrix-matched external calibrations. LOD is defined as 3 times the signal
223 obtained from blank samples.

224

225 **Results**

226 During all measurements animals were engaged in a cognitively demanding task with stable
227 behavioral performance to minimize state dependent fluctuations of basal extracellular
228 concentrations of neuromodulators. Three brain regions were selected to provide a sample of
229 extracellular neuromodulatory concentrations. Two cortical regions: prefrontal cortex (PFC) area
230 8, premotor cortex (PreMC) area 6 and the head of the caudate nucleus (CD) were selected (**Fig**
231 **1F**). In 3 daily sessions, we sampled 3 times per session simultaneously from all three areas.
232 Monkey As had an additional 3 days of recording with one sample collected on each day. Overall
233 we collected and analyzed 12 probes in monkey As and 9 probes in monkey Ke. We were

234 specifically interested in major neuromodulators and neurotransmitters but successfully measured
235 other compounds such as amino acids (e.g. glutamine, taurine, phenylalanine etc) that we do not
236 discuss here.

237 To allow comparison of the SPME extraction results to those typically reported in
238 microdialysis studies, we calculated the relative change in measured concentrations across the
239 three successive sampling events per session pooled across monkeys to enhance the statistical
240 power of the analysis (**Fig 2**). Relative to the end of the first sampling event, the second and third
241 sampling events started after 40 minutes and 100 minutes respectively. We expected that the
242 variability of measurements (indexed as standard error of the median) is comparable to repeatedly
243 measured microdialysis of an identical, active brain state. We found that measured concentrations
244 did not change significantly across sampling events for any compound area combination
245 (Wilcoxon rank sum test; **Fig 2**).

246 We found that four target neurotransmitters and neuromodulators were reliably detected in
247 each animal: glutamate, dopamine, acetylcholine, and choline. Serotonin was also detected on
248 several probes but always near the limit of detection (LOD) and therefore was excluded from
249 analyses here (Lendor et al. 2019). Glutamate concentrations were several orders of magnitude
250 higher than all other observed compounds of interest in all areas and both animals. Relative to
251 glutamate, choline concentrations were >15 times lower, DA concentrations were >700 lower and
252 ACh concentrations were >8300 times lower (**Fig 3**).

253 Glutamate concentrations (across areas), measured as median ± standard error, ranged from
254 159,147 (±19,395) to 233,659 ng/mL (±33,917) in monkey As, and from 135,523 (±22,945) to
255 184,333 ng/mL (±33,516) in monkey Ke. In both monkeys, glutamate concentrations were highest
256 in the head of the caudate, which was significantly different from glutamate concentrations in the

257 premotor cortex in monkey As (kruskal-wallis test with Tukey's HSD correction, p = 0.048) but
258 not in monkey Ke (kruskal-wallis test with Tukey's HSD correction, p = 0.847, n.s.). Glutamate
259 concentrations between the caudate and PFC, as well as the PFC and premotor cortex were not
260 significantly different for either animal. Comparisons between monkeys showed no significant
261 differences between the glutamate concentrations in any of the measured areas (**Fig 3**).

262 In addition to glutamate, dopamine could be reliably detected in both monkeys in the
263 caudate at concentrations of 232 ng/mL (±47) in monkey As, and 226 ng/mL (±31) in monkey Ke.
264 These concentrations were similar between monkeys (Wilcoxon rank sum test p = 1, n.s.).
265 Dopamine was not found above detection limits in frontal cortex.

266 Acetylcholine measurements in the three brain areas ranged from (across areas) 25 (±2) to
267 36 ng/mL (±5) in monkey As, and from 29 (±2) to 36 ng/mL (±4) in monkey Ke. In monkey As,
268 extracellular ACh concentrations between the caudate and premotor cortex were significantly
269 different (kruskal-wallis test with Tukey's HSD correction, p = 0.008). Cortical areas were not
270 significantly different from one another (kruskal-wallis test with Tukey's HSD correction, p =
271 0.476, n.s.) nor was there a significant difference between the caudate and PFC (kruskal-wallis test
272 with Tukey's HSD correction, p = 0.145, n.s.). In monkey Ke, only one cortical region had
273 concentrations of ACh above detection limits, which approached significant difference to the
274 concentrations measured in the caudate (Wilcoxon rank sum test, p = 0.08). Measurements of
275 extracted ACh in the pre-motor cortex of monkey Ke were consistently below detection limits (**Fig**
276 **3**).

277 We also measured choline which is a main product of the enzymatic breakdown of the
278 highly regulated ACh and which is a main indicator of attentional modulation of cholinergic
279 activity in frontal cortex (Parikh et al. 2007). Choline concentrations ranged across areas from

280 2,914 (±590) to 5,078 ng/mL (±675) in monkey As, and 3,408 (±3,705) to 5,533 ng/mL (±860) in
281 monkey Ke. Choline concentrations between the caudate and premotor cortex were significantly
282 different in monkey As (kruskal-wallis test with Tukey's HSD correction, $p = 0.030$), but not in
283 monkey Ke (kruskal-wallis test with Tukey's HSD correction, $p = 0.729$, n.s.). All other area
284 comparisons were not significant for both monkeys. Comparisons of choline concentrations
285 between monkeys were not significant in any of the measured areas.

286 Overall, serotonin concentrations were not observed as reliably as the other reported
287 neurochemicals and therefore were excluded from the main analyses. However, in monkey As,
288 serotonin was observed near the LOD in the prefrontal cortex as well as the caudate in a subset of
289 probes. Within the 9 probes placed in both areas, serotonin was detected in 22% of samples (2/9
290 probes) in the prefrontal cortex and 33% of samples (3/9 probes) in the caudate nucleus. Serotonin
291 observations ranged from 149 ng/mL to 232 ng/mL with a median of 171 ng/mL (±18.5 ng/mL;
292 standard error of the median) with a LOD of 100 ng/mL. The proximity of the measurements to
293 the LOD suggest that the other probes likely collected concentrations of serotonin below the
294 detection threshold. No serotonin observations were made in monkey Ke.

295

296 **Discussion**

297 We demonstrated the reliable measurements of glutamate, dopamine, acetylcholine and choline
298 simultaneously within cortical and subcortical regions of awake and behaving macaques using
299 coated microprobes optimized for solid phase microextraction. Glutamate concentrations were
300 several orders of magnitude higher than dopamine, acetylcholine and choline across brain regions.
301 Extracellular concentrations of choline, dopamine and acetylcholine were detected at >15, >700,
302 and >8,300 times lower than glutamate respectively. Dopamine was readily detected in the caudate

303 but not observed at detectable concentrations in the cortical regions measured. Acetylcholine
304 concentrations showed a statistical trend of being different between the caudate and measured
305 cortical areas and with high consistency between monkeys. Choline concentrations, a product of
306 acetylcholine degradation as well as a precursor for its synthesis, were negatively correlated with
307 acetylcholine ($R = -0.355$; $p = 0.01$). Together, these findings provide new and rare insights about
308 the neurochemical circuit profiles during an active brain state in three areas of the primate fronto-
309 striatal network.

310 The high consistency of measured concentrations within animals, between brain areas and
311 between monkeys suggests that SPME microprobes could provide a versatile neuro-technique for
312 understanding how variations of the neurochemical milieu relate to local and long-range circuit
313 operations and ultimately cognitive functioning.

314

315 **Extracellular Concentrations of Glutamate, Dopamine, Acetylcholine and Choline.** Our
316 results revealed particularly high levels of glutamate within all measured brain regions (PFC,
317 PreMC, and CD) relative to other neuromodulators. This finding is consistent with its ubiquitous
318 role as major excitatory neurotransmitter. This holds true even in the caudate which consists
319 exclusively of GABAergic neurons, but receives glutamatergic inputs from the cortex (Haber and
320 Knutson 2010). Tonic concentrations of glutamate within the striatum have been previously
321 reported to be comparable to that of the hippocampus, prefrontal cortex and other cortical areas
322 due to glutamatergic inputs, extra-synaptic release and glial release (Ascenzo et al. 2006;
323 Moghaddam 1993; Moussawi et al. 2011). In contrast, classical neuromodulators such as DA and
324 ACh, are released in extracellular space through volume transmission where they are highly
325 regulated and may bind to receptors on multiple neurons (Santello et al. 2012; Schwartz and Javitch

326 2013; Syková 2004; Vizi 2000). This regulation may help explain the relatively low observed
327 concentrations of DA and ACh and may be a large source of extracellular choline through the
328 enzymatic breakdown of ACh.

329 Extracellular DA was measured well above the detection threshold in the striatum. In
330 combination with glutamatergic and cholinergic concentrations, our results show promise in the
331 application of SPME to further our understanding of the relationship between glutamatergic inputs
332 to the striatum and the neuromodulatory ACh and DA signals impinging on striatal circuits. Such
333 circuits are strongly involved in hypo- and hyperkinetic diseases (Halliday et al. 2014; Millan et
334 al. 2012). Dopaminergic signals did not exceed the detection threshold in either cortical regions.
335 The presence of DA in the PFC is well documented (Goldman-Rakic et al. 1990; Vijayraghavan
336 et al. 2007; Watanabe et al. 1997) and we thus conclude that DA most likely has failed to exceed
337 our detection limit. The difference between the detection success of DA in the caudate vs PFC and
338 PreM cortex may be due to differences in available DA, release concentrations and dynamics
339 (Holloway et al. 2019). A possible explanation for the lack of detectable cortical DA is the
340 susceptibility of catecholamines to oxidation. This may be partially addressed by faster coupling
341 of sample collection to quantitation by MS.

342 Few previous studies have documented ACh concentrations in vivo in non-human primates
343 due to its rapid breakdown by acetylcholinesterase and the challenges of neurochemical testing in
344 primates (Kreitzer 2009; Schwartz and Javitch 2013; Zapata et al. 2013). ACh plays a major role
345 in organizing local circuits, deployment of attention, locomotion and reward through different
346 receptors present in cortical and subcortical regions (Granger et al. 2016; Howe et al. 2017; Moehle
347 et al. 2017). It has been difficult to discern which ACh concentration corresponds to efficient
348 endogenous circuit operations. Our finding of measurements in all sampling locations except for

349 premotor cortex in monkey Ke, is therefore a promising starting point for future studies comparing
350 ACh concentrations, in conjunction with other neuromodulators, during different cognitive states.
351 The fast turn-around of ACh due to AChE however, likely leads to an underestimation of ACh
352 concentrations by SPME. Although AChE cannot traverse the porous SPME coating due to its size
353 (~7.6nm diameter), preventing any enzymatic degradation of trapped ACh, the dynamic
354 equilibration process continuously leads to a transfer of ACh out of the SPME coating following
355 the concentration gradient of the rapidly depleted ACh into the extracellular space as discussed in
356 the case of calibration in the coating approach (Alam and Pawliszyn 2016; Zhang et al. 2007a).
357 Amongst other sources, choline is created as a byproduct of ACh degradation by AChE.
358 Choline is also a precursor for the synthesis of ACh. Given this relationship, a negative correlation
359 between choline concentrations and ACh is expected which we indeed observed in our dataset.
360 Despite the difference in the measured concentrations of choline and acetylcholine, other studies
361 with similar differences have demonstrated the relationship of ACh and choline to behavior within
362 the cortex (Parikh et al. 2007). Future studies may focus on quantifying this relationship across a
363 wider range of brain states.
364 Many factors may contribute to variation in measured concentrations of neuromodulators
365 including behavioral state, the specific brain region measured and individual differences amongst
366 others. Importantly, different methods may yield different estimates of absolute extracellular
367 concentrations. For example, comparable measurements of extracellular glutamate via MD or
368 voltammetry as opposed to electrophysiological estimates can differ by orders of magnitude and
369 may be attributed to differences in probe size, or sensitivity to different sources of glutamate
370 (Moussawi et al. 2011).
371

372 **Reliable Measurement of Individual Differences of State Specific Neuromodulatory Tone.**
373 Our results suggest that SPME probes provide reliable and sensitive measurements in consecutive
374 sampling events within an experimental session and between sessions on consecutive days. These
375 results were obtained while we controlled brain states across measurement events by engaging
376 animals in a cognitive task. This experimental control could have contributed to the comparable
377 extracellular levels of neuromodulators from sample to sample within *and* between days from
378 similar brain locations (**Fig 2**) (Marder et al. 2014; McGinley et al. 2015; Reimer et al. 2014,
379 2016). The reproducibility of multiple measurements at the same anatomical location within and
380 between days suggests that the SPME penetrations did not significantly disturb tissue (Cudjoe et
381 al. 2013). This conclusion contrasts with reported experience from microdialysis measurements,
382 where the initial placement of the probe or guiding cannula causes transient measurement
383 instabilities that can require several hours of settling time before reliable, steady state
384 neuromodulator concentrations are measurable (Kodama et al. 2002, 2015, 2017; Moussawi et al.
385 2011; Watanabe et al. 1997). These waiting periods must be taken into account when designing
386 microdialysis experiments for in vivo tracking of neuromodulators during behavioral tasks in
387 awake and restrained animals. Furthermore, the reliability of observations for the reported
388 neurochemicals with SPME is extremely high and outperforms many reported microdialysis
389 studies. We present 100% reliability in reporting glutamate and choline concentrations in all brain
390 regions and subjects. Acetylcholine concentrations were reported with 100% reliability in one
391 animal and 92% (11/12 probes) in the other within the prefrontal cortex, 0% reliability (below
392 detection threshold) in one animal and 83% (10/12 probes) in the other within the premotor cortex
393 and 100% reliability in one animal and 92% (11/12 probes) in the other within the caudate.

394 Dopamine concentrations were reported with 100% reliability in both animals in the caudate and
395 were not observed above detection thresholds in the cortex.
396
397 **Qualities and Advantages of SPME.** Our results illustrate several inherent advantages of using
398 SPME to measure neurochemical profiles in brain circuits (Lendor et al. 2019). As illustrated in
399 **Table S1**, SPME complements or outperforms alternative techniques in various domains.
400 Practically, the arbitrary length of the wire where the SPME coating is placed allows for robust
401 placement within the brain. The narrow diameter of the SPME probe that is within the range
402 common to electrodes for electrophysiological recordings, allows for repeated, simultaneous
403 sampling at multiple sites without observable changes to detected extracellular neuromodulator
404 levels using 20-minute sampling times.
405 *Spatial Resolution.* In principle, the spatial resolution of the SPME measurements are
406 capable of reflecting laminar concentration gradients across areas as small as several tens of
407 micrometers. In our protocol we coated 3mm in length with 50 μm of thickness and desorbed the
408 entire area into an organic solvent mixture for subsequent LC-MS/MS analysis. However, with the
409 use of other techniques, such as desorption electrospray ionization (DESI), which represents a
410 direct-to-MS approach (Deng et al. 2014), much smaller areas of the SPME matrix may be
411 analyzed at a time allowing for laminar or near-laminar resolution. Direct coupling of SPME fibres
412 to MS is the preferred mode, as it provides the most rapid analysis thus preventing diffusion of
413 compounds within the coating and smearing the imprinted layer information. If diffusion of
414 molecules within the fibre is high, it can be prevented by, for example, the inclusion of a divider
415 between two halves of the coating. This would allow the simultaneous measurement of separated
416 compartments of a cortical column. The absolute spatial resolution of SPME is difficult to estimate

417 as SPME operates through diffusion and dynamic equilibration similar to MD. As a consequence,
418 the sampled volume will depend on sampling time, the compound's diffusion coefficient, as well
419 as the target tissue and its properties affecting the rate of diffusion such as tortuosity (Syková
420 2004).

421 *Temporal Resolution.* Several factors determine the appropriate extraction time using
422 SPME. Depending on the goals of an experimenter, resolutions below 5 minutes may be achieved
423 as the detection limit is reached within the first few minutes for most compounds tested (**Fig 1D-**
424 **E**). As sampling continues, the SPME coating will eventually reach an equilibrium point with the
425 external environment (**Fig 1D-E**). In principle, sampling times beyond a stable equilibrium point
426 will result in the same extracted values of compounds. However, in the brain there is no single
427 stable equilibrium point and thus, even with long sampling times, there will be some variation in
428 extracted concentrations. Within the dynamic regime, we can still calculate environmental
429 concentrations from which sampling occurred given knowledge of the extraction time and the
430 dynamic range. The lower limit of this dynamic range that can be informative is determined by the
431 coating's physicochemical characteristics and sample's properties and in practice also volume of
432 desorption and sensitivity of the MS. The analytical technique's sensitivity also practically
433 determines the thickness of the SPME coating as thinner coatings could in principle increase
434 temporal resolution but would extract less compounds overall requiring higher sensitivity to detect.
435 With higher sensitivity, less time is required for the thin coating to extract sufficient amounts to
436 exceed limits of detection and quantitation. This then means that the compound with regards to
437 which the sensitivity is the lowest, limits the temporal resolution because it will have the slowest-
438 to-reach detectable concentration. However, making measurements in the dynamic range requires
439 consistency of extraction times as differences in time will lead to variations of extraction yields in

440 a range that can be estimated from the SPME extraction time profiles (**Fig 1D-E**). Given the
441 dynamic nature of brain networks and the lack of a stable equilibrium point, we expect consistency
442 in brain states to be one of the biggest factors in reducing replicated variability. Moreover, SPME
443 measurements are inherently an average of the temporal dynamics of the target tissue milieu. This
444 means that due to the bi-directional exchange of neuromodulators from the extracellular space and
445 the SPME coating, longer periods of stable concentration gradients will be more strongly reflected
446 in the extracted measurements.

447 *Utility and Ease of Use.* SPME based microprobe extraction allows for multiple
448 simultaneous measurements that can be reliably repeated within the same measurement sessions
449 at the same locations with no evidence of damage induced disruption of the neurochemical
450 environment. Another critical advantage of SPME over comparable MS-analysis based methods
451 such as MD is its ease of use and accessibility. Due to their similar size to recording
452 microelectrodes used for electrophysiology, little adjustment is required for conducting SPME
453 measurements using existing acute microelectrode positioning systems. Measurements in deeper
454 structures should use an accompanying guide tube (**Fig 1C**) as travelling through non-target tissue
455 will result in unwanted chemical collection. Beyond the collection, a chemistry core could apply
456 LC-MS/MS to the probes allowing for relatively easy quantitation of extracellular compounds of
457 interest.

458 *Detection Methods.* SPME is ultimately a sampling method, much like MD, that provides
459 data for analytical tools such as chromatography and mass spectrometry. In fact, once SPME
460 analytes have been desorbed from the probe into a solvent, data provided by SPME and MD are
461 treated very much the same. Thus, the advancement in detection limits and reliability of post-hoc
462 analytical methods utilized by MD also benefit SPME, and vice versa. However, SPME sample

463 analysis is more reliably and conveniently coupled to LC-MS/MS as it lacks issues such as high
464 salt content of collected dialysate that MD suffers from (Guihen and Connor 2009).

465 *Extension of SPME measurements beyond classical neuromodulators*. A unique advantage
466 of SPME over alternative methods of in vivo detection of compounds within the brain is its
467 potential affinity for hydrophobic compounds. Although MD is capable of collecting
468 metabolomics data similarly to SPME (Anderzhanova and Wotjak 2013; Li et al. 2012; Zhang et
469 al. 2007b), the artificial cerebra-spinal fluid that is commonly traversing the semi-permeable
470 membrane better facilitates the collection of hydrophilic molecules. This means that molecules
471 that cross the semi-permeable membrane and are therefore collected and quantified through LC-
472 MS are much more likely to be hydrophilic. SPME, in contrast, provides balanced analyte
473 coverage, which means that in principle certain SPME matrix coatings have similar affinity for
474 both hydrophilic or hydrophobic compounds (Reyes-garcés et al. 2018). Data collected here
475 includes other neurochemicals of interest such as amino acids (e.g. glutamine, taurine,
476 phenylalanine, etc) that we reliably detected but do not discuss here. In practice, the detection of
477 very polar molecules such as monoamines and catecholamines requires coating chemistry that
478 facilitates hydrophilic compound extraction. Comparatively many lipids play important roles in
479 intracellular signaling and have been suggested to provide biomarkers for psychiatric disorders
480 (Tamiji and Crawford 2011; Yehuda et al. 1999), therefore making SPME a potentially versatile
481 and comprehensive tool for brain neurochemistry studies.

482

483 **Future direction and improvements to the SPME neurochemical sensing.** The next immediate
484 steps for the continued testing of SPME's utility as a neurochemical sampling method is to evaluate
485 its ability to report behavioral state dependent changes in extracellular neuromodulator

486 concentrations. Similar testing as described here will be conducted with varying, stable behavioral
487 states such as passive engagement, active task engagement, and drowsy/sleepiness. We predict
488 that the various brain regions tested will display different changes in neuromodulator
489 concentrations as a function of behavioral state.

490 Several improvements to the protocol can be made in order to make SPME more
491 informative. Using a more sensitive MS would reduce detection thresholds and increase sensitivity
492 in detecting compounds not successfully measured here such as GABA, serotonin or
493 norepinephrine. This would be very impactful, especially in the case of serotonin for reasons
494 discussed above. Additionally, efforts could be made to improve the extracting phase synthesis
495 and functionalization protocols and increase the extracting capabilities of SPME probes.
496 Moreover, in order to decrease the MS background and interferences in the range of small
497 molecules, derivatization strategy could be considered.

498 For GABA, the most promising strategy is post-desorption derivatization by reagent
499 increasing the compound's hydrophobicity resulting in better MS signal such as benzoyl chloride
500 (Wong 2016). Catecholamine and acetylcholine detection may be improved by optimizing the
501 post-sampling analysis pipeline. Improvements can be made at several steps in order to better
502 preserve and quantify catecholamines: (1) faster coupling of sampling to desorption (2) trying
503 various antioxidant solutions and other preservatives for maintaining catecholamine integrity and
504 (3) faster analysis of the desorbed analytes. Faster coupling of sampling to desorption could be
505 achieved through a more stream-lined process of fibre placement and retraction involving a static
506 cannula maintained through several sampling events. This mechanism would also allow for a faster
507 replacement of SPME probes resulting in a shorter delay between consecutive measurements.

508 A preliminary experiment using both spiked artificial cerebra-spinal fluid (aCSF) and lamb
509 brain homogenate with very high, known concentrations of all target compounds yielded
510 detectable concentrations of all target compounds indicating that the extracting phase of the SPME
511 probe is capable of capturing all compounds of interest. Furthermore, simultaneously collected
512 replicates displayed very little loss of collected compounds over several days within a -80°C
513 freezer (data not shown). Various strategies were compared for storage and placement of extraction
514 fibres in desorption solvent prior to -80°C storage seemed most reliable for many compounds and
515 will be the storage method utilized in the future. Such findings neither support nor antagonize the
516 suggested strategies for improving SPME yield and sensitivity in primates as detection properties
517 within the aCSF and lamb brain homogenate may not accurately reflect those observed in vivo in
518 primates. This is likely contributed to by the dynamic and highly regulated nature of target
519 compounds within the extracellular space of the brain and the dynamic equilibrium between the
520 extracting phase of the SPME probes and the extracellular environment. Further tests of the
521 possible differences between these mediums and improvement strategies to SPME probes are
522 subject for future studies.
523
524 **Implications for Understanding and Treating Psychiatric Disease States.** Most psychiatric
525 disorders are accompanied by neuromodulatory dysregulation (Millan et al. 2012). However, this
526 fact is seldom studied in a multi-modulatory manner with a single or few nuclei or neurochemicals
527 being observed at a time. This is an increasingly evident problem because models attributing
528 symptoms of a disorder to a single neuromodulator often fall short in explaining many symptoms
529 (Bohnen et al. 2015; Remy et al. 2005). For example, in Parkinson's disease, outside of the well
530 characterized dopaminergic deficits, there is evidence for deficits in noradrenergic, cholinergic

531 and serotonergic systems as well (Halliday et al. 1990, 2014; Moehle et al. 2017). Many cognitive
532 deficits observed within Parkinson's disease are linked to such non-dopaminergic deficits. Such
533 findings emphasize the need to simultaneously observe multiple neuromodulatory systems. Thus
534 the simultaneous measurement of multiple neuromodulators, in multiple brain regions within
535 healthy and clinical populations will allow for a better understanding of the underlying causes of
536 symptoms and progression of psychiatric disorders (Anderzhanova and Wotjak 2015; Avery and
537 Krichmar 2017; Millan et al. 2012).

538 A better understanding of psychiatric disorders through multi-modulator methods may also
539 lead to more accurate understanding of the action of pharmacological agents. Previously, many
540 studies aimed at identifying the locus of action of a pharmacological agent have used local
541 injection methods such as iontophoresis or microinjections (Lapiz and Morilak 2006; Wang et al.
542 2007). Although highly informative about the role of neuromodulators in modulating the activity
543 of individual cells and circuits, this approach does not allow physiologically realistic exploration
544 of a systemically administered pharmacological agent. Pharmacological agents are often
545 administered in some systemic fashion and even with highly specific receptor affinities, may
546 interact with multiple neuromodulatory systems through the actions of heteroreceptors (Avery and
547 Krichmar 2017; Gobert et al. 1998; Millan et al. 2015). Multi-modulator measurements, as
548 described here, will allow for a better understanding of pharmacological agents, as well as provide
549 novel insights into the development of more effective drugs or combinations of drugs to better
550 treat the clinical population.

551

552 **Conclusion**. We described a novel SPME protocol capable of simultaneous, multi-modulator
553 measurements of multiple brain regions. Our results suggest that SPME both supplements current

554 methods of neuromodulator detection and allows for novel measurements previously not possible
555 for the investigation and dissection of neuromodulatory systems, their role in physiological brain
556 processes and their modulation by pharmacological agents.
557

558 **Acknowledgments**

559 This research was supported by grants from the Canadian Institutes of Health Research (CIHR),
560 the Natural Sciences and Engineering Research Council of Canada (NSERC) and the Ontario
561 Ministry of Economic Development and Innovation (MEDI). We thank Dr. Hongying Wang for
562 invaluable help with animal care. We thank Thermo Scientifc for providing the triple quadrupole
563 mass spectrometer TSQ Quantiva used in this work as a loan to our laboratory. The authors
564 thankfully acknowledge Pfizer Canada Inc., Merck Canada Inc., Quebec Consortium for Drug
565 Discovery (CQDM), Brain Canada, and Ontario Brain Institute for the grant "Solid phase
566 microextraction-based integrated platform for untargeted and targeted in vivo brain studies".
567

568 **Conflicts of interest**

569 None of the authors have any conflict to disclose.

570 **References**
571
572 **Alam N**, **Pawliszyn J**. Numerical Simulation and Experimental Validation of Calibrant-Loaded
573 Extraction Phase Standardization Approach. *Anal Chem* 88: 8632–8639, 2016.
574 **Anderzhanova E**, **Wotjak CT**. Brain microdialysis and its applications in experimental
575 neurochemistry. *Cell Tissue Res* 354: 27–39, 2013.
576 **Anderzhanova E**, **Wotjak CT**. NextGen Brain Microdialysis : Applying Modern Metabolomics
577 Technology to the Analysis of Extracellular Fluid in the Central Nervous System. *Mol*
578 *Neuropsychiatry* 1: 60–67, 2015.
579 **Arnsten AFT**, **Paspalas CD**, **Gamo NJ**, **Yang Y**, **Wang M**. Dynamic network connectivity: A
580 new form of neuroplasticity. *Trends Cogn Sci* 14: 365–375, 2010.
581 **Ascenzo MD**, **Fellin T**, **Terunuma M**, **Revilla-sanchez R**, **Meaney DF**, **Auberson YP**, **Moss**
582 **SJ**, **Haydon PG**. mGluR5 stimulates gliotransmission in the nucleus accumbens. *Proc Natl Acad*
583 *Sci* 104: 1995–2000, 2006.
584 **Avery MC**, **Krichmar JL**. Neuromodulatory Systems and Their Interactions : A Review of
585 Models , Theories , and Experiments. *Front Neural Circuits* 11: 1–18, 2017.
586 **Bohnen NB**, **Albin R**, **Muller MLTM**, **Petrou M**, **Kotagal V**, **Koeppe RA**, **Scott PJH**, **Frey**
587 **KA**. Frequency of Cholinergic and Caudate Nucleus Dopaminergic Deficits Across the
588 Predemented Cognitive Spectrum of Parkinson Disease and Evidence of Interaction Effects.
589 *JAMA Neurol* 72: 194–200, 2015.
590 **Buck K**, **Voehringer P**, **Ferger B**. Rapid analysis of GABA and glutamate in microdialysis
591 samples using high performance liquid chromatography and tandem mass spectrometry. *J*
592 *Neurosci Methods* 182: 78–84, 2009.
593 **Cudjoe E**, **Bojko B**, **de Lannoy I**, **Saldivia V**, **Pawliszyn J**. Solid-Phase Microextraction: A
594 Complementary In Vivo Sampling Method to Microdialysis. *Angew Chemie Int Ed* 52: 12124–
595 12126, 2013.
596 **Cudjoe E**, **Pawliszyn J**. Optimization of solid phase microextraction coatings for liquid
597 chromatography mass spectrometry determination of neurotransmitters. *J Chromatogr A* 1341:
598 1–7, 2014.
599 **Dale N**, **Hatz S**, **Tian F**, **Llaudet E**. Listening to the brain: Microelectrode biosensors for
600 neurochemicals. *Trends Biotechnol* 23: 420–428, 2005.
601 **Deng J**, **Yang Y**, **Wang X**, **Luan T**. Strategies for coupling solid-phase microextraction with
602 mass spectrometry. *TrAC - Trends Anal Chem* 55: 55–67, 2014.
603 **Disney AA**, **McKinney C**, **Grissom L**, **Lu X**, **Reynolds JH**. A multi-site array for combined
604 local electrochemistry and electrophysiology in the non-human primate brain. *J Neurosci*
605 *Methods* 255: 29–37, 2015.
606 **Fisher RE**, **Morris ED**, **Alpert NM**, **Fischman AJ**. In Vivo Imaging of Neuromodulatory
607 Synaptic Transmission Using PET : A Review of Relevant Neurophysiology. *Hum Brain Mapp*
608 3: 24–34, 1995.
609 **Ghersi C**, **Bonfanti A**, **Manzari B**, **Feligioni M**, **Raiteri M**, **Pittaluga A**. Pharmacological
610 heterogeneity of release-regulating presynaptic AMPA / kainate receptors in the rat brain : study
611 with receptor antagonists. *Neurochem Int* 42: 283–292, 2003.
612 **Gobert A**, **Audinot V**, **Cistarelli L**, **Millan MJ**. Simultaneous quantification of serotonin,
613 dopamine and noradrenaline levels in single frontal cortex dialysates of freely-moving rats
614 reaveals a complex pattern of reciprocal auto- and heteroreceptor-mediated control of release.
615 *Neuroscience* 84: 413–429, 1998.

616 **Goldman-Rakic PS**, **Lidow MS**, **Gallager DW**. Overlap of dopaminergic, adrenergic, and
617 serotoninergic receptors and complementarity of their subtypes in primate prefrontal cortex. *J*
618 *Neurosci* 10: 2125–2138, 1990.
619 **Gómez-Ríos GA**, **Tascon M**, **Reyes-garcés N**, **Boyacı E**. Quantitative analysis of biofluid spots
620 by coated blade spray mass spectrometry , a new approach to rapid screening. *Sci Rep* 7: 1–7,
621 2017.
622 **Granger AJ**, **Mulder N**, **Saunders A**, **Sabatini BL**. Cotransmission of acetylcholine and
623 GABA. *Neuropharmacology* 100: 40–46, 2016.
624 **Grilli M**, **Zappettini S**, **Zanardi A**, **Lagomarsino F**, **Pittaluga A**, **Zoli M**, **Marchi M**.
625 Exposure to an enriched environment selectively increases the functional response of the pre-
626 synaptic NMDA receptors which modulate noradrenaline release in mouse hippocampus. *J*
627 *Neurochem* 110: 1598–1606, 2009.
628 **Guihen E**, **Connor WTO**. Current separation and detection methods in microdialysis the drive
629 towards sensitivity and speed. *Electrophoresis* 30: 2062–2075, 2009.
630 **Haber SN**, **Knutson B**. The reward circuit: Linking primate anatomy and human imaging.
631 *Neuropsychopharmacology* 35: 4–26, 2010.
632 **Halliday GM**, **Leverenz JB**, **Schneider JS**, **Adler CH**. The Neurobiological Basis of Cognitive
633 Impairment in Parkinson's Disease. *Mov Disord* 29: 634–650, 2014.
634 **Halliday GM**, **Li YW**, **Blumbergs PC**, **Joh TH**, **Cotton PRGH**, **Howe PRC**, **Blessing WW**,
635 **Geffen LB**. Neuropathology of Immunohstochemically Idendied Brainstem Neurons in
636 Parkinson's Disease. *Am Neurol Assoc* 27: 373–385, 1990.
637 **Hassan SF**, **Zumut S**, **Burke PG**, **Mcmullan S**, **Cornish JL**, **Goodchild AK**. Comparison of
638 noradrenlaine, dopamine and serotonin in mediating the tachycardic and thermogenic effects of
639 methamphetamine in the ventral medial prefrontal cortex. *Neuroscience* 295: 209–220, 2015.
640 **Hassani SA**, **Oemisch M**, **Balcarras M**, **Westendorff S**, **Ardid S**, **van der Meer MA**, **Tiesinga**
641 **P**, **Womelsdorf T**. A computational psychiatry approach identifies how alpha-2A noradrenergic
642 agonist Guanfacine affects feature-based reinforcement learning in the macaque. *Sci Rep* 7:
643 40606, 2017.
644 **Holloway ZR**, **Freels TG**, **Comstock JF**, **Nolen HG**, **Sable HJ**, **Lester DB**. Comparing phasic
645 dopamine dynamics in the striatum, nucleus accumbens, amygdala, and medial prefrontal cortex.
646 *Synapse* 73: 1–15, 2019.
647 **Howe WM**, **Gritton HJ**, **Lusk NA**, **Roberts EA**, **Hetrick VL**, **Berke JD**, **Sarter M**.
648 Acetylcholine Release in Prefrontal Cortex Promotes Gamma Oscillations and Theta–Gamma
649 Coupling during Cue Detection. *J Neurosci* 37: 3215–3230, 2017.
650 **Jacobs CB**, **Peairs MJ**, **Venton BJ**. Review: Carbon nanotube based electrochemical sensors
651 for biomolecules. *Anal Chim Acta* 662: 105–127, 2010.
652 **Kennedy RT**. Emerging trends in in vivo neurochemical monitoring by microdialysis. *Curr*
653 *Opin Chem Biol* 17: 860–867, 2013.
654 **Kodama T**, **Hikosaka K**, **Honda Y**, **Kojima T**, **Tsutsui K**, **Watanabe M**. Dopamine and
655 glutamate release in the anterior default system during rest : A monkey microdialysis study.
656 *Behav Brain Res* 294: 194–197, 2015.
657 **Kodama T**, **Hikosaka K**, **Watanabe M**. Differential changes in glutamate concentration in the
658 primate prefrontal cortex during spatial delayed alternation and sensory-guided tasks. *Exp Brain*
659 *Res* 145: 133–141, 2002.
660 **Kodama T**, **Kojima T**, **Honda Y**, **Hosokawa T**, **Tsutsui K**, **Watanabe M**. Oral Administration
661 of Methylphenidate (Ritalin) Affects Dopamine Release Differentially Between the Prefrontal

662 Cortex and Striatum: A Microdialysis Study in the Monkey. *J Neurosci* 37: 2387–2394, 2017.
663 **König M**, **Thinnes A**, **Klein J**. Microdialysis and its use in behavioural studies: Focus on
664 acetylcholine. *J Neurosci Methods* 300: 206–215, 2018.
665 **Kreitzer AC**. Physiology and pharmacology of striatal neurons. *Annu Rev Neurosci* 32: 127–47,
666 2009.
667 **Lapiz MDS**, **Morilak DA**. Noradrenergic modulation of cognitive function in rat medial
668 prefrontal cortex as measured by attentional set shifting capability. *Neuroscience* 137: 1039–
669 1049, 2006.
670 **Lendor S**, **Hassani S-A**, **Boyaci E**, **Singh V**, **Womelsdorf T**, **Pawliszyn J**. Solid Phase
671 Microextraction-Based Miniaturized Probe and Protocol for Extraction of Neurotransmitters
672 from Brains in Vivo. *Anal Chem* 91: 4896–4905, 2019.
673 **Li J**, **von Pföstl V**, **Zaldivar D**, **Zhang X**, **Logothetis NK**, **Rauch A**. Measuring multiple
674 neurochemicals and related metabolites in blood and brain of the rhesus monkey by using dual
675 microdialysis sampling and capillary hydrophilic interaction chromatography-mass spectrometry.
676 *Anal Bioanal Chem* 402: 2545–2554, 2012.
677 **Luccini E**, **Musante V**, **Neri E**, **Brambilla Bas M**, **Severi P**, **Raiteri M**, **Pittaluga A**.
678 Functional interactions between presynaptic NMDA receptors and metabotropic glutamate
679 receptors co-expressed on rat and human noradrenergic terminals. *Br J Pharmacol* 151: 1087–
680 1094, 2007.
681 **Marder E**. Overview Neuromodulation of Neuronal Circuits: Back to the Future. *Neuron* 76: 1–
682 11, 2012.
683 **Marder E**, **O'Leary T**, **Shruti S**. Neuromodulation of Circuits with Variable Parameters: Single
684 Neurons and Small Circuits Reveal Principles of State-Dependent and Robust Neuromodulation.
685 *Annu Rev Neurosci* 37: 329–346, 2014.
686 **McGinley MJ**, **Vinck M**, **Reimer J**, **Batista-Brito R**, **Zagha E**, **Cadwell CR**, **Tolias AS**,
687 **Cardin JA**, **McCormick DA**. Waking State: Rapid Variations Modulate Neural and Behavioral
688 Responses. *Neuron* 87: 1143–1161, 2015.
689 **Millan MJ**, **Agid Y**, **Brüne M**, **Bullmore ET**, **Carter CS**, **Clayton NS**, **Connor R**, **Davis S**,
690 **Deakin B**, **DeRubeis RJ**, **Dubois B**, **Geyer MA**, **Goodwin GM**, **Gorwood P**, **Jay TM**, **Joëls**
691 **M**, **Mansuy IM**, **Meyer-Lindenberg A**, **Murphy D**, **Rolls E**, **Saletu B**, **Spedding M**, **Sweeney**
692 **J**, **Whittington M**, **Young LJ**. Cognitive dysfunction in psychiatric disorders: characteristics,
693 causes and the quest for improved therapy. *Nat Rev Drug Discov* 11: 141–168, 2012.
694 **Millan MJ**, **Goodwin GM**, **Meyer-lindenberg A**, **Ove S**. Learning from the past and looking to
695 the future : Emerging perspectives for improving the treatment of psychiatric disorders. *Eur*
696 *Neuropsychopharmacol* 25: 599–656, 2015.
697 **Moehle MS**, **Pancani T**, **Byun N**, **Yohn SE**, **Wilson GH**, **Dickerson JW**, **Remke DH**, **Xiang**
698 **Z**, **Niswender CM**, **Wess J**, **Jones CK**, **Lindsley CW**, **Rook JM**, **Conn PJ**. Cholinergic
699 Projections to the Substantia Nigra Pars Reticulata Inhibit Dopamine Modulation of Basal
700 Ganglia through the M4Muscarinic Receptor. *Neuron* 96: 1358–1372, 2017.
701 **Moghaddam B**. Stress Preferentially Increases Extraneurona Levels of Excitatory Amino Acids
702 in the Prefrontal Cortex : Comparison to Hippocampus and Basal Ganglia. *J Neurochem* 60:
703 1650–1657, 1993.
704 **Moussawi K**, **Riegel A**, **Nair S**, **Kalivas PW**, **Bargas J**, **Nacional U**. Extracellular glutamate :
705 functional compartments operate in different concentration ranges. *Front Syst Neurosci* 5: 1–9,
706 2011.
707 **Oemisch M**, **Westendorff S**, **Oemisch M**, **Westendorff S**, **Everling S**, **Womelsdorf XT**.

Interareal Spike-Train Correlations of Anterior Cingulate and Dorsal Prefrontal Cortex during Attention Shifts Interareal Spike-Train Correlations of Anterior Cingulate and Dorsal Prefrontal Cortex during Attention Shifts. *J Neurosci* 35: 13076–13089, 2015.

Ouyang G, **Pawliszyn J**. Configurations and calibration methods for passive sampling techniques. *J Chromatogr A* 1168: 226–235, 2007.

Parikh V, **Kozak R**, **Martinez V**, **Sarter M**. Prefrontal Acetylcholine Release Controls Cue Detection on Multiple Timescales. *Neuron* 56: 141–154, 2007.

Pawliszyn J. Theory of Solid-Phase Microextraction. *J Chromatogr Sci* 38: 270–278, 2000.

Pawliszyn J. Theory of Solid-Phase Microextraction. In: *Handbook of Solid Phase Microextraction*, edited by Pawliszyn J. Elsevier, 2012, p. 13–59.

Paxinos G, **Huang X**, **Toga A**. *The Rhesus Monkey Brain in Stereotaxic Coordinates*. 2000.

Perry M, **Li Q**, **Kennedy RT**. Review of recent advances in analytical techniques for the determination of neurotransmitters. *Anal Chim Acta* 653: 1–22, 2009.

Pittaluga A. Presynaptic release-regulating mGlu1 receptors in central nervous system. *Front Pharmacol* 7: 1–15, 2016.

Pittaluga A, **Feligioni M**, **Longordo F**, **Luccini E**, **Raiteri M**. Trafficking of presynaptic AMPA receptors mediating neurotransmitter release : Neuronal selectivity and relationships with sensitivity to cyclothiazide. *Neuropharmacology* 50: 286–296, 2006.

Quintero JE, **Day BK**, **Zhang Z**, **Grondin R**, **Stephens ML**, **Huettl P**, **Pomerleau F**, **Gash DM**, **Gerhardt GA**. Amperometric measures of age-related changes in glutamate regulation in the cortex of rhesus monkeys. *Exp Neurol* 208: 238–246, 2007.

Reimer J, **Froudarakis E**, **Cadwell CR**, **Yatsenko D**, **Denfield GH**, **Tolias AS**. Pupil Fluctuations Track Fast Switching of Cortical States during Quiet Wakefulness. *Neuron* 84: 355–362, 2014.

Reimer J, **McGinley MJ**, **Liu Y**, **Rodenkirch C**, **Wang Q**, **McCormick DA**, **Tolias AS**. Pupil fluctuations track rapid changes in adrenergic and cholinergic activity in cortex. *Nat Commun* 7: 1–7, 2016.

Remy P, **Doder M**, **Lees A**, **Turjanski N**, **Brooks D**. Depression in Parkinson ' s disease: loss of dopamine and noradrenaline innervation in the limbic system. *Brain* 128: 1314–1322, 2005.

Reyes-garcés N, **Gionfriddo E**, **Gómez-Ríos GA**, **Alam MN**, **Boyaci E**, **Bojko B**, **Singh V**, **Grandy J**, **Pawliszyn J**. Advances in Solid Phase Microextraction and Perspective on Future Directions. *Anal Chem* 90: 302–360, 2018.

Santana N, **Mengod G**, **Artigas F**. Expression of a1-adrenergic receptors in rat prefrontal cortex: cellular co-localization with 5-HT2A receptors. *Int J Neuropsychopharmacol* 16: 1139–1151, 2018.

Santello M, **Calì C**, **Bezzi P**. Gliotransmission and the Tripartite Synapse. In: *Synaptic Plasticity. Advances in Experimental Medicine and Biology*, edited by Kreutz M, Sala C. 2012, p. 307–331.

Schluter EW, **Mitz AR**, **Cheer JF**, **Averbeck BB**. Real-time dopamine measurement in awake monkeys. *PLoS One* 9, 2014.

Schwartz J, **Javitch J**. Neurotransmitters. In: *Principles of Neural Science*, edited by Kandel E, Schwartz J, Jessell T, Siegelbaum S, Hudspeth A. 2013, p. 289–306.

Schwerdt HN, **Shimazu H**, **Amemori K**, **Amemori S**, **Tierney PL**, **Gibson DJ**, **Hong S**, **Yoshida T**, **Langer R**, **Cima MJ**, **Graybiel AM**. Long-term dopamine neurochemical monitoring in primates. *Proc Natl Acad Sci* 114: 13260–13265, 2017.

Syková E. Extrasynaptic volume transmission and diffusion parameters of the extracellular

space. *Neuroscience* 129: 861–876, 2004.
Tamiji J, **Crawford A**. The Neurobiology of Lipid Metabolism in. *Eur PMC* 18: 98–112, 2011.
Thiele A, **Bellgrove MA**. Neuromodulation of Attention. *Neuron* 97: 769–785, 2018.
Vartak D, **Togt C Van Der**, **Vugt B Van**, **Roelfsema PR**. Electrochemical measurement of acetylcholine in the dorsolateral prefrontal cortex : A technical report. *BioRXiv* 1–25, 2017.
Vijayraghavan S, **Wang M**, **Birnbaum SG**, **Williams G V.**, **Arnsten AFT**. Inverted-U dopamine D1 receptor actions on prefrontal neurons engaged in working memory. *Nat Neurosci* 10: 376–384, 2007.
Vizi ES. Role of high-affinity receptors and membrane transporters in nonsynaptic communication and drug action in the central nervous system. *Pharmacol Rev* 52: 63–89, 2000.
Wang JKT, **Andrews H**, **Thukral V**. Presynaptic Glutamate Receptors Regulate Noradrenaline Release from Isolated Nerve Terminals. *J Neurochem* 58: 204–211, 1992.
Wang M, **Ramos BP**, **Paspalas CD**, **Shu Y**, **Simen A**, **Duque A**, **Vijayraghavan S**, **Brennan A**, **Dudley A**, **Nou E**, **Mazer J a.**, **McCormick D a.**, **Arnsten a. FT**. alpha2A-Adrenoceptors Strengthen Working Memory Networks by Inhibiting cAMP-HCN Channel Signaling in Prefrontal Cortex. *Cell* 129: 397–410, 2007.
Watanabe M, **Kodama T**, **Hikosaka K**. Increase of Extracellular Dopamine in Primate Prefrontal Cortex During a Working Memory Task. *J Neurophysiol* 78: 2795–2798, 1997.
Watson CJ, **Venton BJ**, **Kennedy RT**. In Vivo Measurements of Neurotransmitters by Microdialysis Sampling. *Anal Chem* 78: 1391–1399, 2006.
Yehuda S, **Rabinovitz S**, **Mostofsky DI**. Mini-Review Essential Fatty Acids Are Mediators of Brain Biochemistry and Cognitive Functions. *J Neurosci Res* 56: 565–570, 1999.
Yoshimi K, **Kumada S**, **Weitemier A**, **Jo T**, **Inoue M**. Reward-induced phasic dopamine release in the monkey ventral striatum and putamen. *PLoS One* 10: 1–22, 2015.
Zapata A, **Chefer VI**, **Parrot S**, **Denoroy L**. Detection and Quantification of Neurotransmitters in Dialysates. *Curr Protoc Neurosci* 63: 1–35, 2013.
Zhang X, **Es-haghi A**, **Musteata FM**, **Ouyang G**, **Pawliszyn J**. Quantitative in Vivo Microsampling for Pharmacokinetic Studies Based on an Integrated Solid-Phase Microextraction System. *Anal Chem* 79: 4507–4513, 2007a.
Zhang X, **Rauch A**, **Lee H**, **Xiao H**, **Rainer G**, **Logothetis N**. Capillary hydrophilic interaction chromatography/mass spectrometry for simultaneous determination of multiple neurotransmitters in primate cerebral cortex. *Rapid Commun Mass Spectrom* 21: 3621–3628, 2007b.

Fig 1. SPME sampling procedure, extraction time profiles and measurement locations. (A) Dimensions of the SPME probe and the accompanying cannula. There was a 3000 µm buffer from the opening of the cannula and the start of the SPME coating. The SPME coating spanned 195 µm at the tip. The SPME coating made up the terminal 3000 µm of the entire probe and was placed in a cannula with an internal diameter of 200 µm and an external diameter of 270 µm. (B) Tungsten microelectrodes were lowered into the brain guided by 3 T magnetic resonance (MR) images in order to map the depth at which detectable spiking was observed matching expectations from the MR images. (C) SPME probes and their accompanying cannulas in all brain areas were then simultaneously lowered to 200 µm above the point of first observable firing in the target brain region and the SPME probes were lowered to expose only the 3000 µm SPME coating. After 20 minutes of extraction, the SPME probes were then retracted 3000 µm back into the cannula and the probes plus their accompanying cannulas were removed from the brain. The table inset into the figure provides the velocities and times of each probe and cannula as they transitioned between the extraction steps. (D) In vitro extraction quantities of Glutamate in ng and (E) Dopamine in ng over time utilized to select in vivo extraction times. The linear "kinetic" regime and "equilibrium" regime are labelled with the dynamic range being in between. (F**)** Anatomical locations of SPME sampling events in the right hemisphere of two Rhesus Macaques. Target brain regions are highlighted in red and include two cortical regions, prefrontal cortex (PFC) area 8 and premotor cortex (PreM) area 6 as well as a subcortical region: the head of the caudate.

Fig 2. Changes in SPME sampling over time.
Changes in the normalized concentrations of the observed neuromodulators across daily sampling sessions in each sampled brain region. The median concentration of (A) Glutamate (B) acetylcholine (C) choline and dopamine (D) with standard error of the median plotted for each sampling time and location. Data was normalization for each subject separately and for the respective neurochemical and area combinations. Sampling locations are represented by different lines: solid line for the prefrontal cortex, dashed line for the premotor cortex and dotted line for the caudate nucleus. Sampling events were 20 minutes in length and the time between the end of one sampling event to the start of the next sampling event was 40 minutes (STD 2 minutes) making the second sampling event 40 minutes and the third 100 minutes from the initial measurement. No significant change was observed for any neuromodulator in any brain region (Wilcoxon rank sum test). Note that a single prefrontal choline data point was excluded in this analysis for being >4 standard deviations from the median (data point is present in **Fig 3a**).

Fig 3. SPME sampling of the macaque brain.
SPME probes extract from the cortex (PFC and PreM6) as well as the caudate of two adult macaques after 20 minutes of extraction within the respective brain region. Median and standard error of the median of n= 12 probes for animal As and n= 9 probes for animal Ke with no data excluded. Four neuromodulators were reliably measured: glutamate, dopamine, acetylcholine, and choline (orange, green, purple, red respectively). All brain regions had high concentrations of glutamate and relatively much lower concentrations of acetylcholine and choline extracted (with the exception of animal Ke PreM6 lacking detectable acetylcholine). The only tested region to yield measurable dopamine was the caudate. The dashed blue line depicts the limit of detection (LOD).

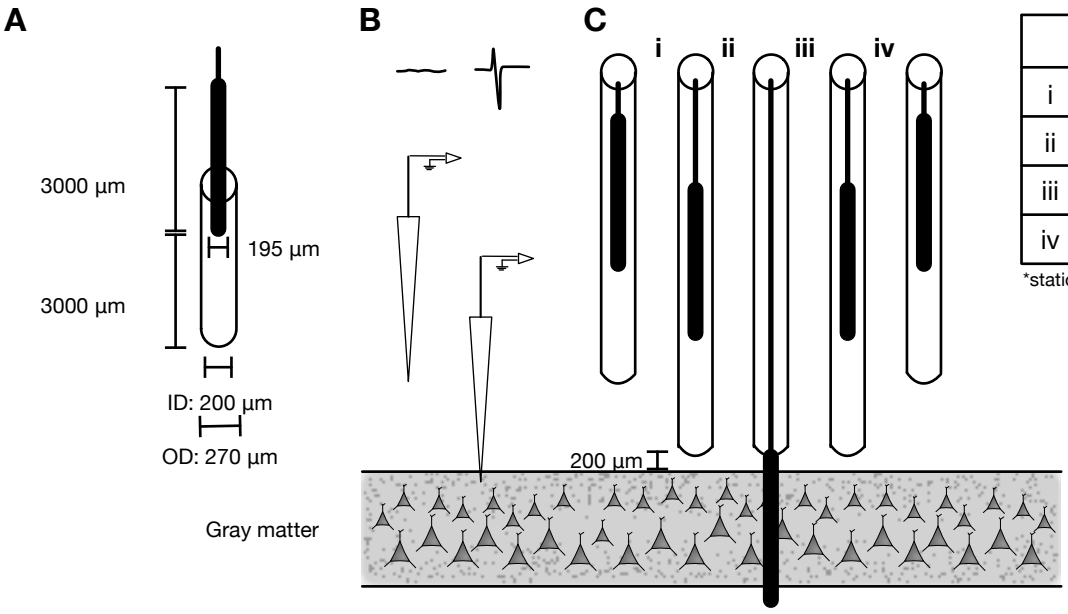

	fibre	cannula	time
i	30 µm/s	30 µm/s	variable
ii	30 µm/s	-	200s
iii	30 µm/s	-	1200s* + 200s
iv	30 µm/s	30 µm/s	variable

*stationary: extraction period of 20 min

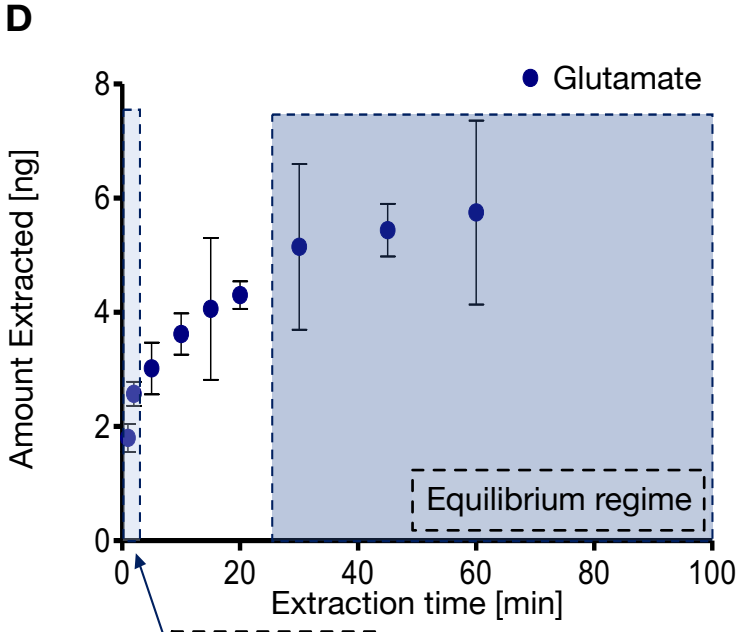

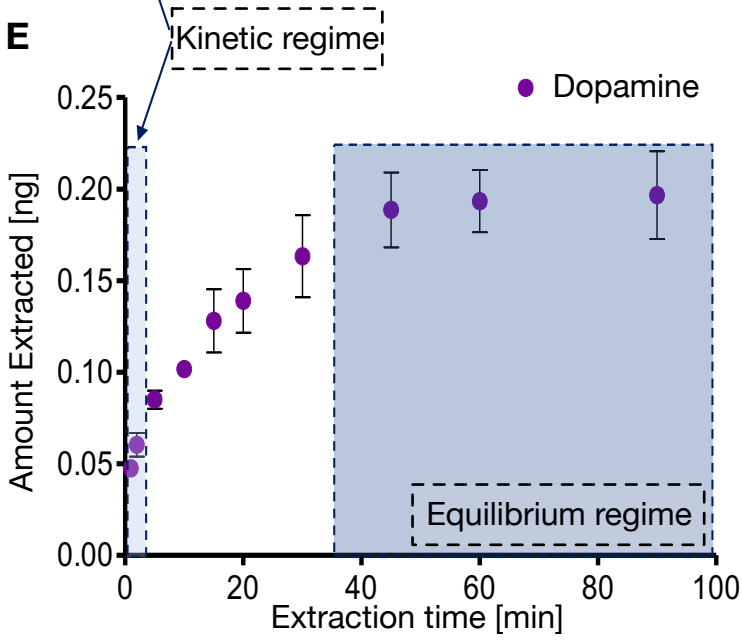

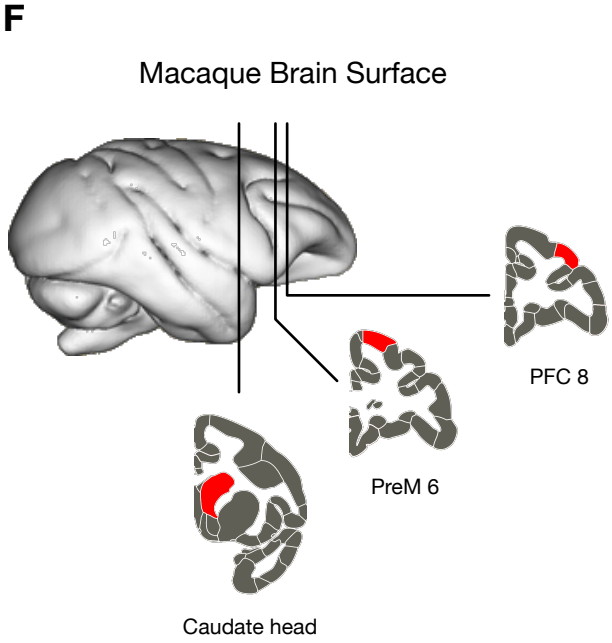

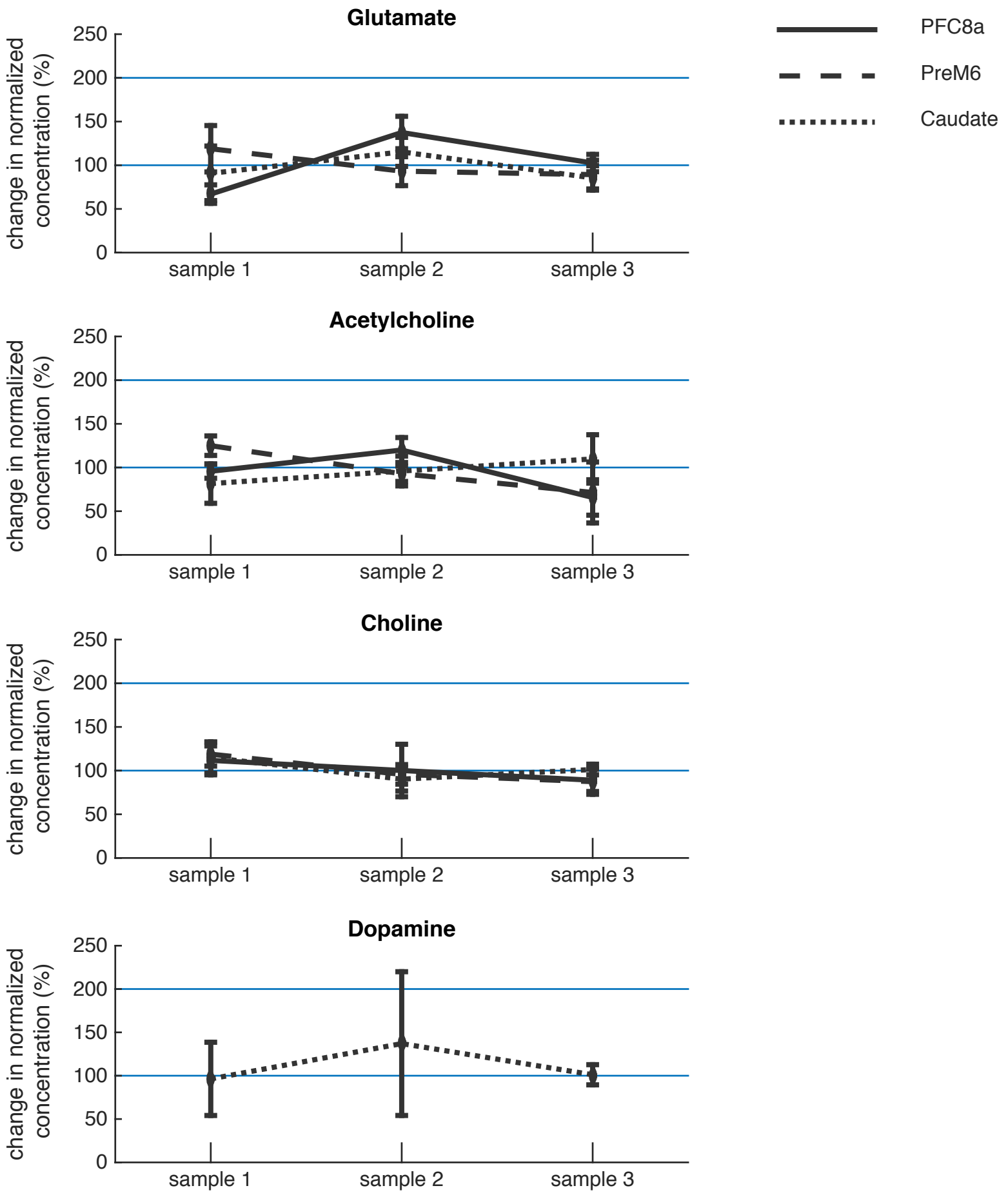
Glutamate
Acetylcholine
Choline
Dopamine
change in normalized concentration (%)
250
200
150
100
50
0
sample 1
sample 2
sample 3
PFC8a
PreM6
Caudate

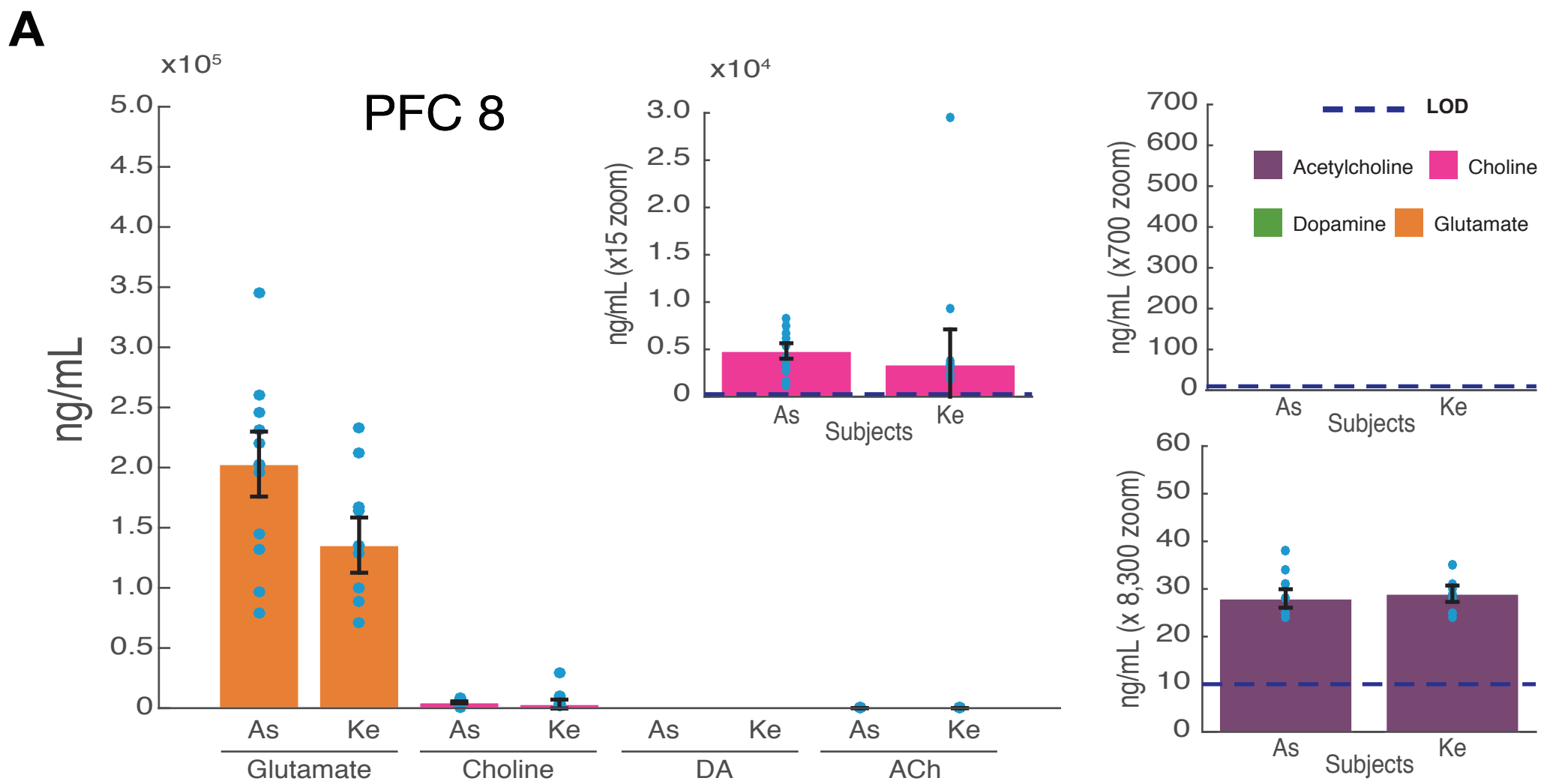
A
PFC 8
x10⁵
ng/mL
5.0
4.5
4.0
3.5
3.0
2.5
2.0
1.5
1.0
0.5
0
As
Ke
Glutamate
Choline
DA
ACh
x10⁴
ng/mL (x15 zoom)
Subjects
LOD
Acetylcholine
Choline
Dopamine
Glutamate
ng/mL (x700 zoom)
ng/mL (x 8,300 zoom)

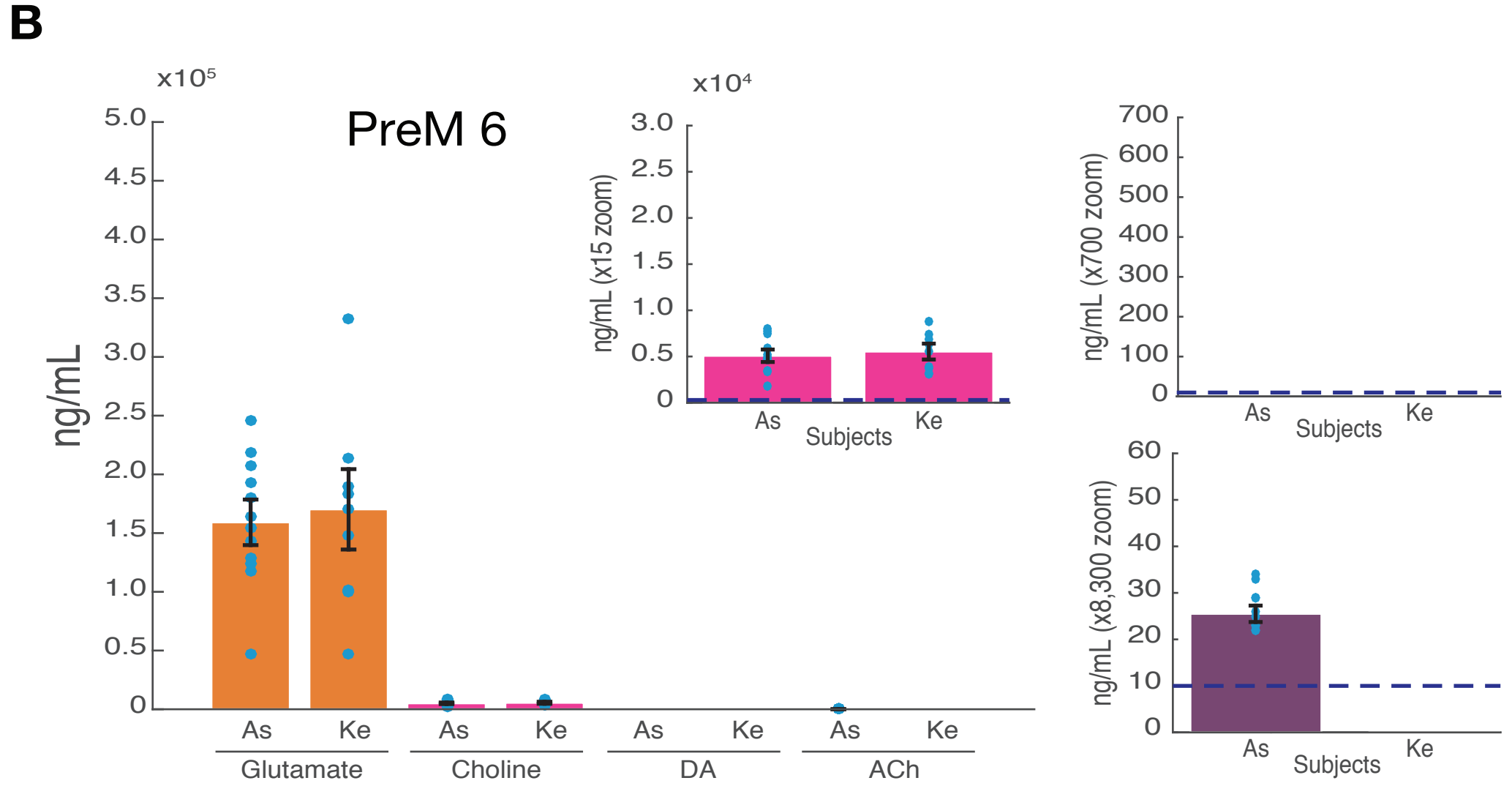
B
PreM 6
x10⁵
ng/mL
5.0
4.5
4.0
3.5
3.0
2.5
2.0
1.5
1.0
0.5
0
As
Ke
Glutamate
Choline
DA
ACh
x10⁴
ng/mL (x15 zoom)
Subjects
ng/mL (x700 zoom)
ng/mL (x8,300 zoom)

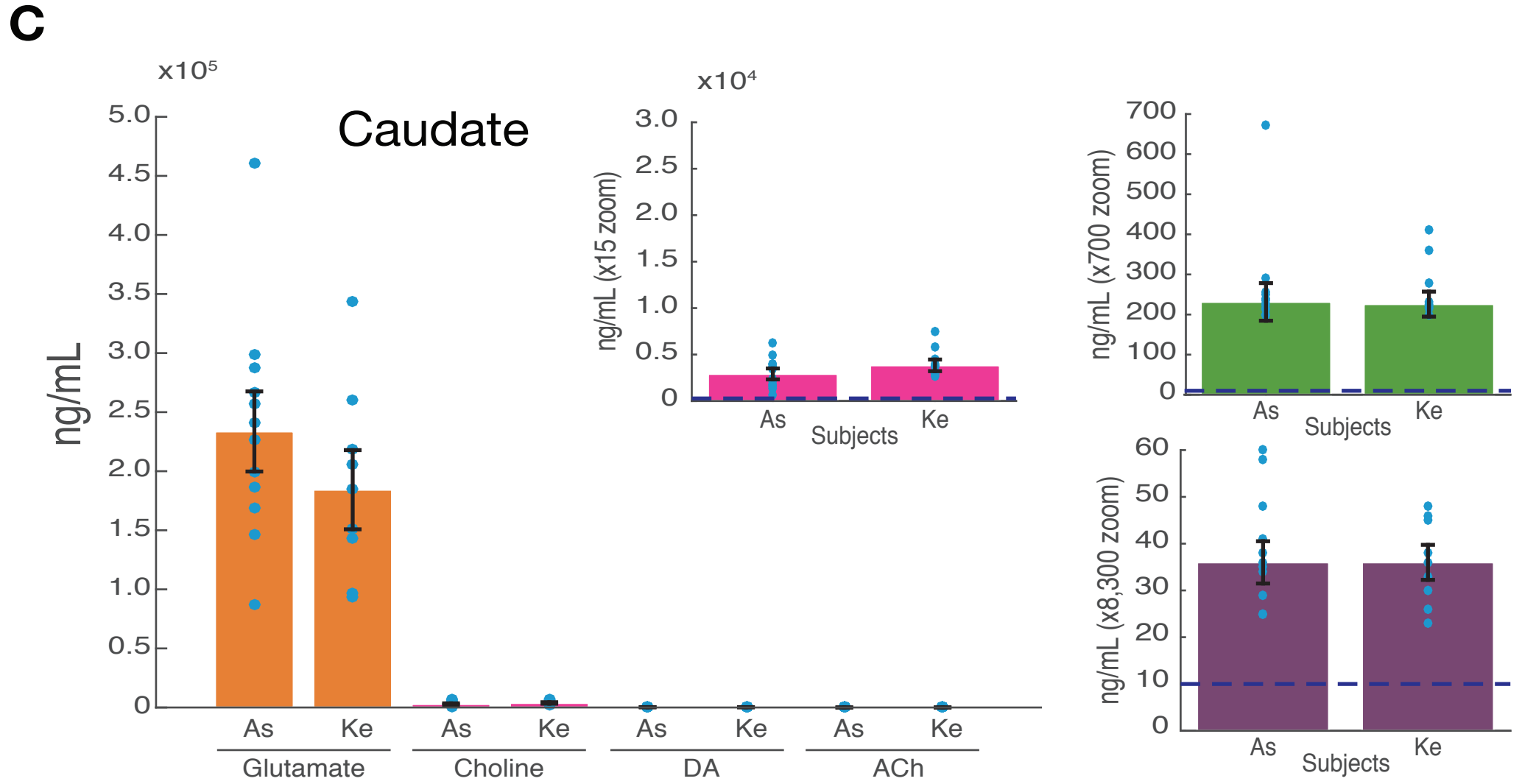
C
Caudate
x10⁵
ng/mL
5.0
4.5
4.0
3.5
3.0
2.5
2.0
1.5
1.0
0.5
0
As
Ke
Glutamate
Choline
DA
ACh
x10⁴
ng/mL (x15 zoom)
Subjects
ng/mL (x700 zoom)
ng/mL (x8,300 zoom)

Supplementary Methods

Chemicals, Reagents and Materials

The LC-MS-grade solvents methanol (MeOH), acetonitrile (ACN), isopropanol (IPA) and water, as well as the acetylcholinesterase inhibitor phenylmethylsulfonyl fluoride (PMSF) were purchased from Fisher Scientifc. Formic acid, polyacrylonitrile (PAN), N,N-dimethylformamide (DMF) and the standards of neurotransmitters: γ-aminobutyric acid (GABA), glutamic acid (Glu), acetylcholine (ACh), histamine (Hist), serotonin (5-HT), dopamine (DA) and choline (Cho) as well as their deuterated analogues were purchased from Millipore Sigma (Oakville, ON, Canada). Epinephrine (Epi), norepinephrine (NE) and their deuterated analogues were obtained from Cerilliant Corporation (Round Rock, TX, USA). Choline-D9, was purchased from Cambridge Isotope Laboratories (Tewksbury, MA, USA). The reagents used for synthesis of hydrophilic-lipophilic balance polymer particles functionalized with strong cation exchange groups, as well as compounds for preparation of PBS were purchased from Millipore-Sigma. The stainless steel wire (stainless steel grade AISI 304, 150 µm diameter) used for manufacturing of SPME probes was purchased from Unimed S.A. (Lausanne, Switzerland). The stainless steel tubing used as guiding cannulas (270 µm O.D.; 200±5 µm I.D.) was obtained from Vita Needle (Needham, MA, USA).

LC-MS/MS Analysis

On the day of analysis, the SPME probes were defrosted and desorbed into 40 µL of water/ACN/MeOH 40:30:30 (v/v/v) mixture containing 1 % of formic acid and a mixture of deuterated isotopologues of targeted neuromodulators (used as internal standards, IS) at 20 ng/mL. The desorption was carried out for 1 h with agitation at 1500 rpm. The extracts were injected into the LC-MS system for targeted neurotransmitter analysis within a few hours after desorption. All experiments were carried out using an Ultimate 3000RS HPLC system coupled to TSQ Quantiva triple quadrupole mass spectrometer (Thermo Fisher Scientific, San Jose, California, USA). Data processing was performed using Thermo software Xcalibur 4.0 and Trace Finder 4.1. For chromatographic separation of the target compounds, a modified method of what is previously reported (Cudjoe and Pawliszyn 2014) was used, adjusted to include more targeted neuromodulators and their corresponding IS. A Kinetex® PFP LC column (100 x 2.1 mm, 1.7 µm; Phenomenex, Torrance, CA, USA) was held at 30°C with the mobile phase flow rate at 400

µL/min. The mobile phase A consisted of water/MeOH/ACN 90:5:5 (v/v/v) with 0.1 % formic acid, and mobile phase B was ACN/water 90:10 (v/v) with 0.1% of formic acid. The chromatographic gradient was applied starting from 100% B for 1 min and increasing the aqueous mobile phase A to 100% for 3 min with convex gradient function, held for 0.5 min and subsequent linear return to initial conditions and re-equilibration for 1 min, yielding total time of 6.5 min. The injection volume was 10 µL. MS/MS analysis was performed with electrospray ionization in positive mode under selected reaction monitoring conditions, with two MS/MS transitions for each neuromodulator (quantifier and qualifier) and one for each IS.

Quantitation of neuromodulators

Individual stock standard solutions of all targeted neuromodulators were prepared in methanol or water with 0.1% formic acid at a concentration of 1 mg/mL and stored at −80 °C for maximum of one month. In order to calculate the amounts of neuromodulators extracted by each probe, calibrator standards prepared in the same desorption solvent as real samples were analyzed in the same batch. This instrumental calibration curve was prepared in the range of 0.1-200 ng/mL by a serial dilution of the stock standard mixture of all compounds at 1µg/mL. The IS concentration was kept constant at 20 ng/mL in all calibrators, identically as in the real samples. The amounts extracted were calculated based on linear regression equation obtained from the analytical signal (the ratio of chromatographic peak areas of analytes and their corresponding IS) plotted against the concentration.

In order to calculate the concentrations of neuromodulators in brain, matrix-matched external calibration approach was used. The surrogate matrix consisted of 2% agar gel mixed with brain homogenate in the ratio 1:1 (*v/w)*. The homogenized brain tissue was earlier incubated with 1 mM PMSF for 1 h at 37°C to prevent enzymatic digestion of acetylcholine in the calibrator samples. Due to several target compounds being present in brain homogenate at high concentrations (e.g. for glutamate and choline the “blank” brain homogenate matrix doesn’t exist), their quantitation was based on signals of their deuterated isotopologues. The calibrator samples were prepared in the surrogate matrix with concentrations of neuromodulators ranging from 5 to 3000 µg/mL for the isotopically labelled compounds or from 10 to 2000 ng/mL for the remaining compounds.

The extractions were carried out with SPME probes manufactured and pre-treated identically to the probes used for *in vivo* sampling and using the same 20 min extraction time and desorption conditions as for the real samples. The amounts of neuromodulators extracted from the calibrator samples were determined in the same way as described above and plotted against concentrations of calibrators. The resulting weighted linear regression equations were applied to the amounts of neuromodulators extracted from the *in vivo* samples, yielding values of concentrations of the compounds of interest in brain.

The limits of detection (LOD) were estimated as the levels corresponding to the signal to noise ratio of 3 and were calculated based on the signal of blank calibrator sample (considered as the noise).

Supplementary Figures

Fig S1. Behavioral task that the monkeys were engaged in. Briefly, the monkey was expected to fixate a central fixation point until criterion when two graded stimuli appeared. The graded stimuli acquired color and motion, of the graded stripes, features in either order. The two stimuli then either simultaneously dimmed (go-signal), or dimmed one at a time in either order. The monkey, through trial and error, identified the rewarded stimulus via its color feature which was the sole identifying feature informative of reward. The monkey was then expected to wait until the dimming of the selected stimulus and respond in the same direction as the motion of the graded stripes on the chosen stimulus. If the monkey correctly accomplished this, it would receive deterministic reward in the form of liquid juice. Monkey As was engaged in a variation of this task with reduced complexity in order to match monkey Ke in performance and reward acquisition over the sampling period. Figure reproduced from Hassani et al., 2017.

Fig S2. Experimental procedure from SPME probe fabrication to quantitation. Fabrication described the in-house procedure to prepare SPME probes. Preparation describes experimental set-up. Sampling describes the actual data collection process. LC/MS analysis describes the chemical quantitation of collected data samples.

Supplementary Tables

Table S1. Overview of in vivo neurochemical measurement methods

	PET imaging	**Electro-chemistry**	**Micro-dialysis**	**Solid phase micro-extraction**
Temporal Resolution	Minutes	Highest (millisecond range)	1-30 minutes; dependent on MS sensitivity, target etc.	<5-30 minutes; dependent on MS sensitivity, coating thickness, target etc.
Spatial Resolution	Voxel	High; surface area may vary (relevant for enzyme based methods)	Diffusion based; surface area may vary	Diffusion based; surface area may vary
Sensitivity	Indirect measurement via competitive radiolabeled species	High	Depending on post-hoc methods (i.e. MS)	Depending on post-hoc methods (i.e. MS)
Neuro-active targets	A few at most	A few at most	Many	Many
Non-neuro-active targets	No	No	Yes, greater efficacy for hydrophilic compounds	Yes, greater potential efficacy for hydrophobic compounds
In vivo feasibility	Difficult in awake, behaving animal models; movement highly restricted	Good (low reliability in NHPs)	Good, often requires chronic implant of cannula for repeated measurements	Very good; robust placement of multiple simultaneous probes and repeatable acute measurements
Cost	High	Requires special equipment	Requires special equipment	Easy to port to an acute micro-electrode setup; requires a chemistry core

Table S1. A comparison of methods capable of measuring single or multiple neurochemicals in vivo. Temporal resolution, spatial resolution, sensitivity, capability to measure neuro-active and non-neuro-active compounds, in vivo feasibility and cost. PET: positron emission tomography; NHP: non-human primate; MS: mass spectrometer.

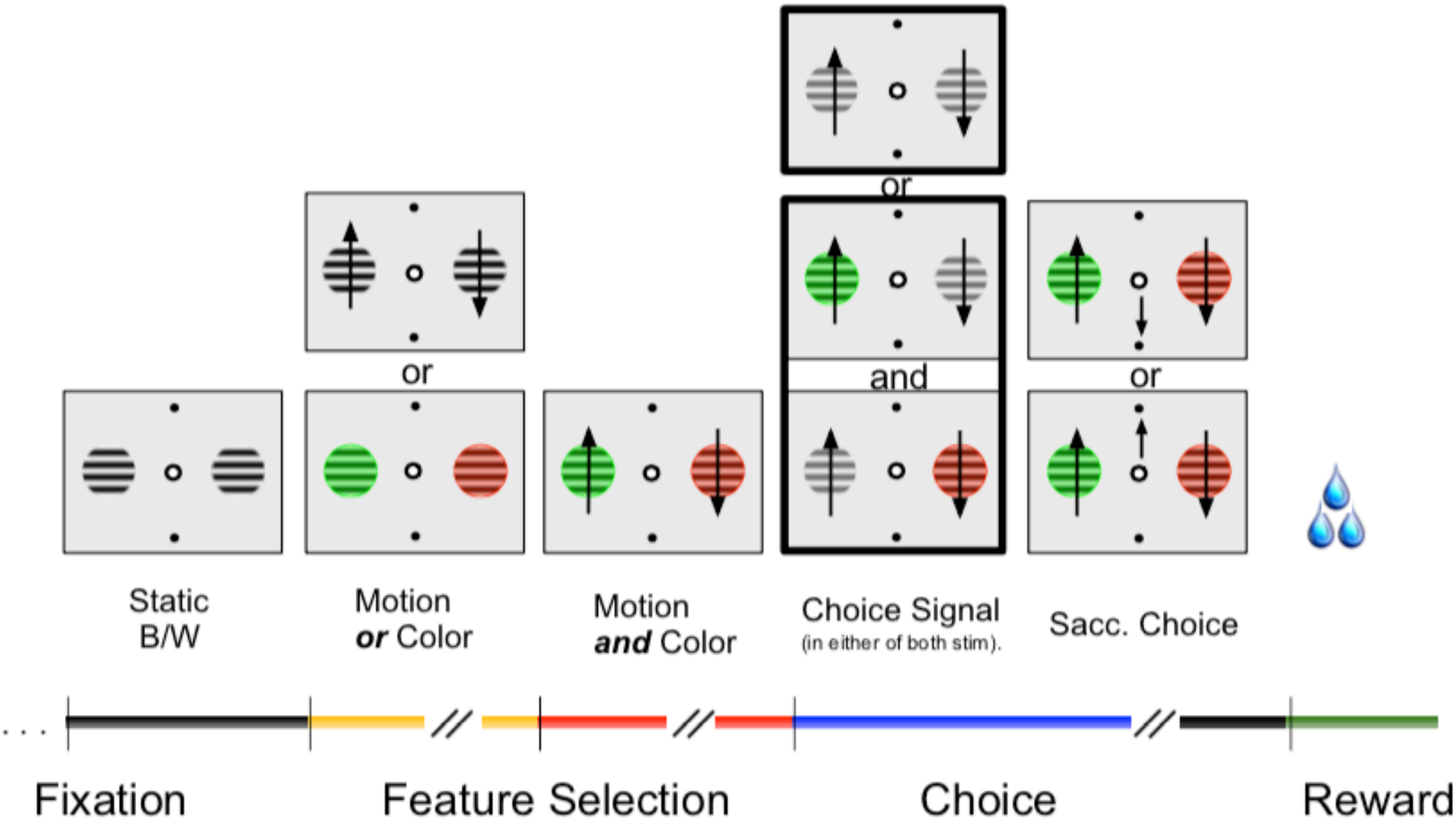
or
or
and
or
Static
B/W
Motion
or Color
Motion
and Color
Choice Signal
(in either of both stim).
Sacc. Choice
Fixation
Feature Selection
Choice
Reward

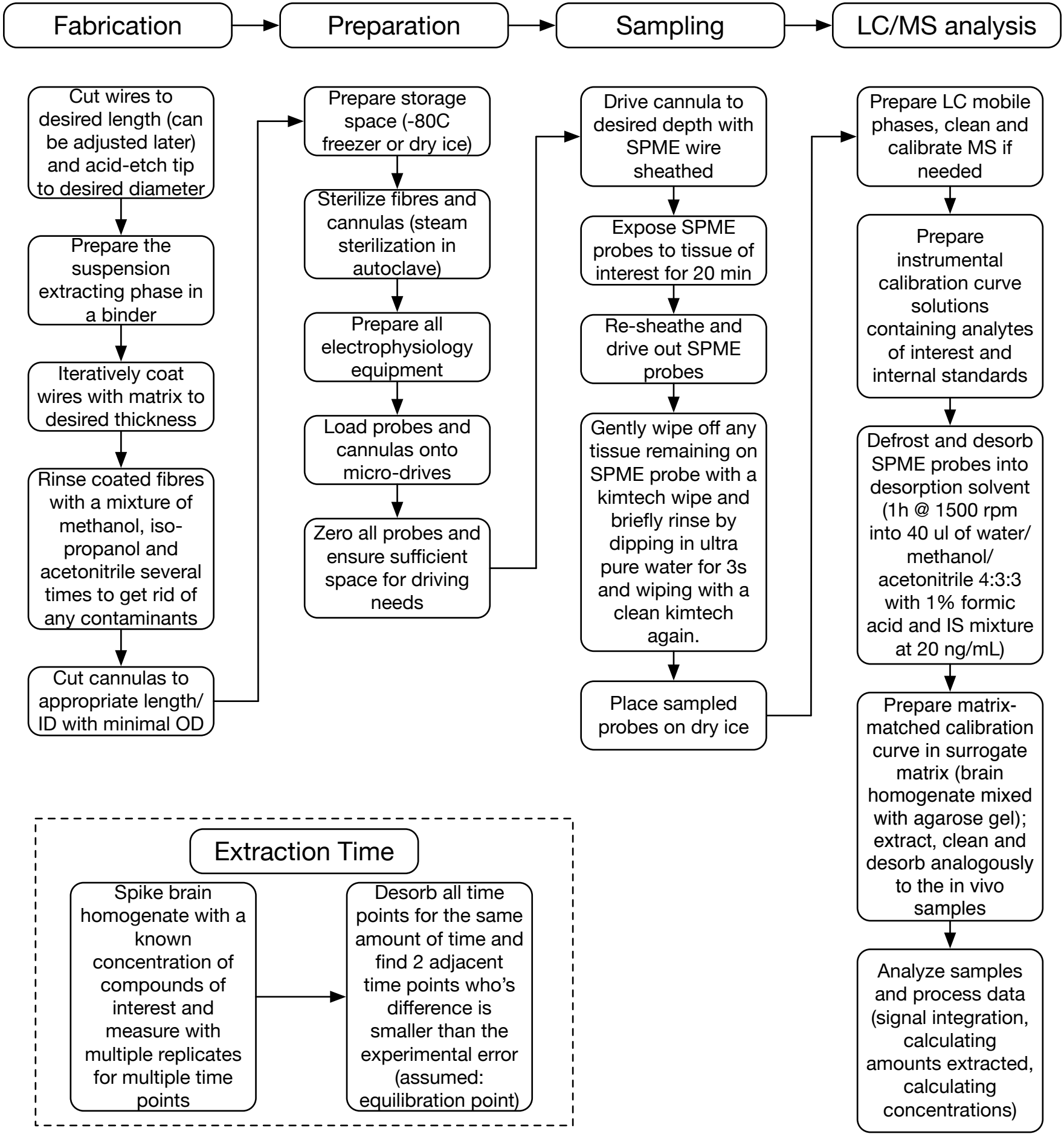
Fabrication
Preparation
Sampling
LC/MS analysis
Cut wires to desired length (can be adjusted later) and acid-etch tip to desired diameter
Prepare the suspension extracting phase in a binder
Iteratively coat wires with matrix to desired thickness
Rinse coated fibres with a mixture of methanol, iso-propanol and acetonitrile several times to get rid of any contaminants
Cut cannulas to appropriate length/ ID with minimal OD
Prepare storage space (-80C freezer or dry ice)
Sterilize fibres and cannulas (steam sterilization in autoclave)
Prepare all electrophysiology equipment
Load probes and cannulas onto micro-drives
Zero all probes and ensure sufficient space for driving needs
Drive cannula to desired depth with SPME wire sheathed
Expose SPME probes to tissue of interest for 20 min
Re-sheathe and drive out SPME probes
Gently wipe off any tissue remaining on SPME probe with a kimtech wipe and briefly rinse by dipping in ultra pure water for 3s and wiping with a clean kimtech again.
Place sampled probes on dry ice
Prepare LC mobile phases, clean and calibrate MS if needed
Prepare instrumental calibration curve solutions containing analytes of interest and internal standards
Defrost and desorb SPME probes into desorption solvent (1h @ 1500 rpm into 40 ul of water/ methanol/ acetonitrile 4:3:3 with 1% formic acid and IS mixture at 20 ng/mL)
Prepare matrix-matched calibration curve in surrogate matrix (brain homogenate mixed with agarose gel); extract, clean and desorb analogously to the in vivo samples
Analyze samples and process data (signal integration, calculating amounts extracted, calculating concentrations)
Extraction Time
Spike brain homogenate with a known concentration of compounds of interest and measure with multiple replicates for multiple time points
Desorb all time points for the same amount of time and find 2 adjacent time points who's difference is smaller than the experimental error (assumed: equilibration point)